Gas Network Modeling: An Overview (Extended English Version)

Pia Domschke[1], Jan Giesselmann[1], Jens Lang[1],
Tobias Breiten[2], Volker Mehrmann[2], Riccardo Morandin[2],
Benjamin Hiller[3], Caren Tischendorf[4]

February 22, 2023

4

With this overview we want to provide a compilation of different models for the description of gas flow in networks in order to facilitate the introduction to the topic. Special attention is paid to the hierarchical structure inherent to the modeling, and the detailed description of individual components such as valves and compressors. Also included are network model classes based on purely algebraic relations, and energy-based port-Hamiltonian models. A short overview of basic numerical methods and concepts for the treatment of hyperbolic balance equations is also given. We do not claim completeness and refer in many places to the existing literature.

The idea of a model catalog came to us in the context of the application for the CRC/Transregio 154 "Mathematical modeling, simulation and optimization using the example of gas networks". The present English translation is an extension from [11]. At this point we would like to thank the DFG for its support.

[1]Technische Universität Darmstadt, Fachbereich Mathematik, Dolivostraße 15, 64293 Darmstadt, {domschke,giesselmann,lang}@mathematik.tu-darmstadt.de
[2]Technische Universität Berlin, Institut für Mathematik, Straße des 17. Juni 136, 10623 Berlin, {breiten,mehrmann,morandin}@math.tu-berlin.de
[3]Konrad-Zuse-Institut Berlin, Takustraße 7, 14195 Berlin, hiller@zib.de
[4]Humboldt Universität zu Berlin, Institut für Mathematik, Rudower Chaussee 25, 12489 Berlin, tischendorf@math.hu-berlin.de

Contents

1 Introduction

There are many different mathematical models for individual components of gas networks. In the following, we briefly present these models in order to reflect the current state of research. Exemplarily for gas, different model hierarchies within the isothermal and the temperature-dependent models are given, including the simplifying assumptions. We also give a short overview of existing discretization methods for the numerical solution of hyperbolic balance laws. Physical and technical fundamentals of gas networks are described in particular in [20, Chapter 2]. In this book, further questions on the evaluation of gas network capacities can be found as well.

2 The Euler Equations

The Euler equations are a system of nonlinear hyperbolic partial differential equations that describe the behavior of compressible, inviscid fluids. They consist of the continuity equation, the momentum equation and the energy equation. In addition, the equation of state applies to real gases. The full Euler equations are (see [5, 24, 39]):

$$\begin{aligned} \frac{\partial \rho}{\partial t} + \frac{\partial}{\partial x}(\rho v) &= 0, \\ \frac{\partial}{\partial t}(\rho v) + \frac{\partial}{\partial x}(p + \rho v^2) &= -\frac{\lambda}{2D}\rho v\,|v| - g\rho\sin(\alpha), \\ \frac{\partial}{\partial t}\left(\rho(\tfrac{1}{2}v^2 + e)\right) + \frac{\partial}{\partial x}\left(\rho v(\tfrac{1}{2}v^2 + e) + pv\right) &= -\frac{k_w}{D}\left(T - T_w\right), \end{aligned} \tag{TA1}$$

together with the equation of state for real gases, $p = R\rho T z(p,T)$. Here ρ denotes the density, v the velocity of the gas, T the temperature and p the pressure. Further, g is the gravitational constant, α is the inclination angle of the gas pipe relative to the level, λ is the pipe friction coefficient, D is the pipe diameter, k_w is the thermal conductivity coefficient, $T_w = T_w(x)$ is the surface temperature of the pipe wall, R is the gas constant, and $z = z(p,T)$ is the compressibility factor. The variable $e = c_v T + gh$ denotes the internal energy (= thermal + potential energy). Here c_v is the specific heat and h is the height above ground. A short derivation of the equations is given e.g. in [2]. Depending on which model is chosen for the compressibility factor, one can resolve the equation of state according to the pressure p and insert it into the equations. The conservation or balance quantities in this system are the density ρ, the mass flux $q = \rho v$, and the total energy $E = \rho(\frac{1}{2}v^2 + e)$.

In [15, p. 141] it is described how mixtures can also be modeled. For this purpose, the system (TA1) is interpreted for the mixture of two components and for the second component a conservation equation with mass fraction Y is added (the first component has then fraction $1 - Y$),

$$\frac{\partial}{\partial t}(\rho Y) + \frac{\partial}{\partial x}(\rho Y v) = 0\,. \tag{1}$$

This can be formulated in an analogous way for mixtures of more than two components.

There are three characteristics to the equations (TA1) which belong to the eigenvalues of the Jacobian matrix of the flux function, see [39, table p. 347]. The eigenvalues are

$$\lambda_1 = v - c\,, \qquad \lambda_2 = v\,, \qquad \lambda_3 = v + c\,. \tag{2}$$

Here, c is the speed of sound. It is generally calculated from $c^2 = \frac{\partial p}{\partial \rho}$ (at constant entropy). In natural gas, it is about $340\,\mathrm{m\,s^{-1}}$. The first and third characteristic families are genuinely nonlinear, whereas the second characteristic family is linearly degenerate. In the linearly degenerate case, contact discontinuities occur. The characteristics are decisive for how or with which velocity information is transported in the gas and which boundary conditions may be set in which way. For the isothermal case (T = const.), see e.g. [12], more generally in [15].

In the following two sections, two parameters of the Euler equations will be explained in more detail: the compressibility factor z, which enters into the equation of state for real gases, and the pipe friction coefficient λ.

2.1 Equation of State for Real Gases

The equation of state for ideal gases is

$$p = R\rho T. \tag{3}$$

However, real gases deviate from this equation of state, which requires a correction with the compressibility factor $z = z(p,T)$. The equation of state is then

$$p = R\rho T z(p,T). \tag{4}$$

For ideal gases, we have $z = 1$. The compressibility factor depends on the chemical composition of the gas as well as on pressure and temperature. For low pressures and high temperatures, real gases behave approximately ideal. At higher pressures, real gases sometimes deviate considerably from the behavior of ideal gases, see Figure 1.

A special model to describe the compressibility factor is used by the American Gas Association (AGA) (see AGA Report No. 8), which is a good approximation for pressures up to 70 bar, see for example [2, 36]. It reads

$$z(p,T) = 1 + 0.257\frac{p}{p_c} - 0.533\frac{pT_c}{p_c T}. \tag{5}$$

Here p_c and T_c are the pseudocritical pressure and the pseudocritical temperature, respectively, which in turn depend on the mixture of the gas [2]. For isothermal equations (T constant), (5) simplifies to

$$z(p) = 1 + \alpha p \qquad \text{with } \alpha = \frac{0.257}{p_c} - 0.533\frac{T_c}{p_c T}. \tag{6}$$

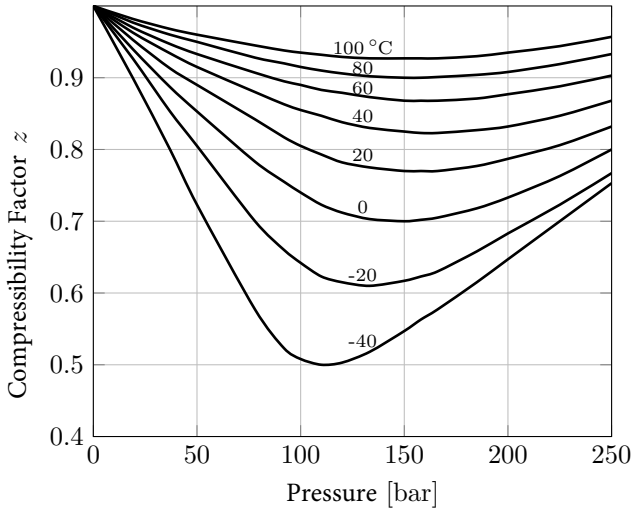

Figure 1: Compressibility factor z of natural gas with standard density $\rho_0 = 0.776\,\mathrm{kg\,m^{-3}}$, according to [35].

Another model to describe the real gas factor is the formula of Papay [33], see also [36],

$$z(p,T) = 1 - 3.52\frac{p}{p_c}\exp\Big(-2.26\frac{T}{T_c}\Big) + 0.274\Big(\frac{p}{p_c}\Big)^2\exp\Big(-1.878\frac{T}{T_c}\Big), \tag{7}$$

which provides good results up to a pressure of 150 bar.

In [32], different equations of state are considered. Osiadacz and Chaczykowski conclude that the selection of the equation of state has only a minor influence on the result of the simulation. In contrast, the pipe friction coefficient, for which there are various calculation models, has a major influence [32].

2.2 The Pipe Friction Coefficient

In addition to the pipe roughness k (in m), the key parameter in the calculation of the pipe friction coefficient is the Reynolds number Re. It is calculated from

$$\mathrm{Re} = \frac{\rho v D}{\eta}. \tag{8}$$

The dynamic viscosity η depends on the type of fluid and is about $10^{-5}\,\mathrm{Pa\,s}$ for natural gas [2].

The magnitude of the Reynolds number indicates whether the flow is laminar or turbulent. Below a critical Reynolds number Re_u (laminar-turbulent transition), the flow is laminar. [40] specifies the critical Reynolds number as 2320. In [37] it is described that the transition from laminar to turbulent flow takes place in a region above a Reynolds

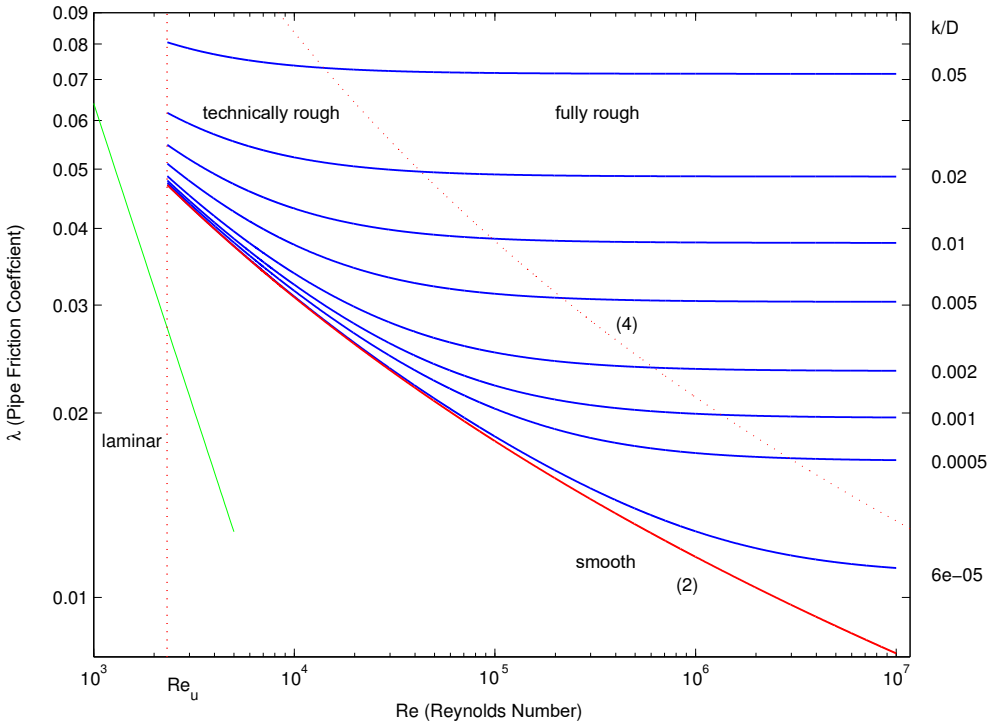

Figure 2: Moody diagram

number of 2000, which cannot be determined in more detail. If the pipe wall is smooth, it can be shown that the pipe friction depends only on the Reynolds number for both laminar and turbulent flow. However, if the pipe wall is fully rough (in fluid mechanical terms), the pipe friction coefficient λ depends only on the relative pipe roughness k/D. The dependence of the pipe friction coefficient on the pipe roughness and the Reynolds number is often shown in the so-called Moody diagram, see Figure 2.

2.2.1 Laminar Flow

Below the critical Reynolds number Re_u, the flow is laminar (Hagen-Poiseuille flow). The velocity profile is parabolic for this flow, see Figure 3. The pipe friction coefficient λ in this case is calculated from

$$\lambda = \frac{64}{\mathrm{Re}}, \tag{9}$$

see [37, 40]. In the Moody diagram (Figure 2), the pipe friction coefficient in the case of laminar flow is shown as a green line (curve on the far left).

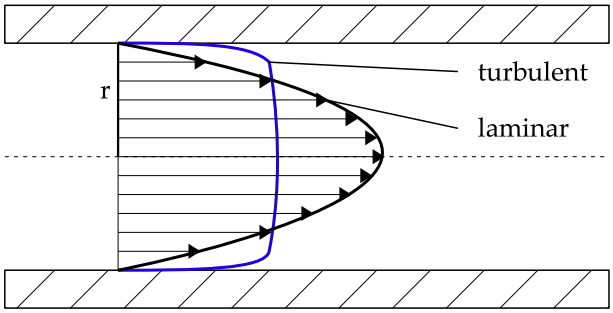

Figure 3: Velocity distribution for laminar and turbulent pipe flow

2.2.2 Turbulent Flow

In turbulent flow, the velocity profile is significantly flattened because the layers flowing side by side constantly mix with each other (see Figure refabb:geschwindigkeitsverteilung). In this case, a distinction is made between hydraulically smooth, technically rough and fully rough pipes.

Hydraulically smooth pipe: Here different models exist for the calculation of λ, e.g. the Blasius correlation

$$\lambda = (100\,\mathrm{Re})^{-\frac{1}{4}}, \tag{10}$$

which, however, is only suitable for Reynolds numbers smaller than 10^5. Further there is the approximate formula of Prandtl or Kármán and Prandtl [37]

$$\frac{1}{\sqrt{\lambda}} = 2\log_{10}\left(\mathrm{Re}\sqrt{\lambda}\right) - 0.8. \tag{11}$$

This implicit formula is suitable for all Reynolds numbers in the turbulent range. The course of the curve is shown in red in the Moody diagram (Figure 2) and marked with (2).

Technically rough pipe: In the transition region between smooth and fully rough pipe wall, the law of Colebrook or Colebrook-White

$$\frac{1}{\sqrt{\lambda}} = -2\log_{10}\left(\frac{2.5226}{\mathrm{Re}\sqrt{\lambda}} + \frac{\frac{k}{D}}{3.7065}\right) \tag{12}$$

is generally used. The pipe friction coefficient is plotted in blue for different values of k/D in the Moody diagram (Figure 2).

The formula of Chen [7] from 1979

$$\frac{1}{\sqrt{\lambda}} = -2\log_{10}\left(\frac{\frac{k}{D}}{3.7065} - \frac{5.0425}{\mathrm{Re}}\log_{10}\left[\frac{(\frac{k}{D})^{1.1098}}{2.8257} + \frac{5.8506}{\mathrm{Re}^{0.8981}}\right]\right) \tag{13}$$

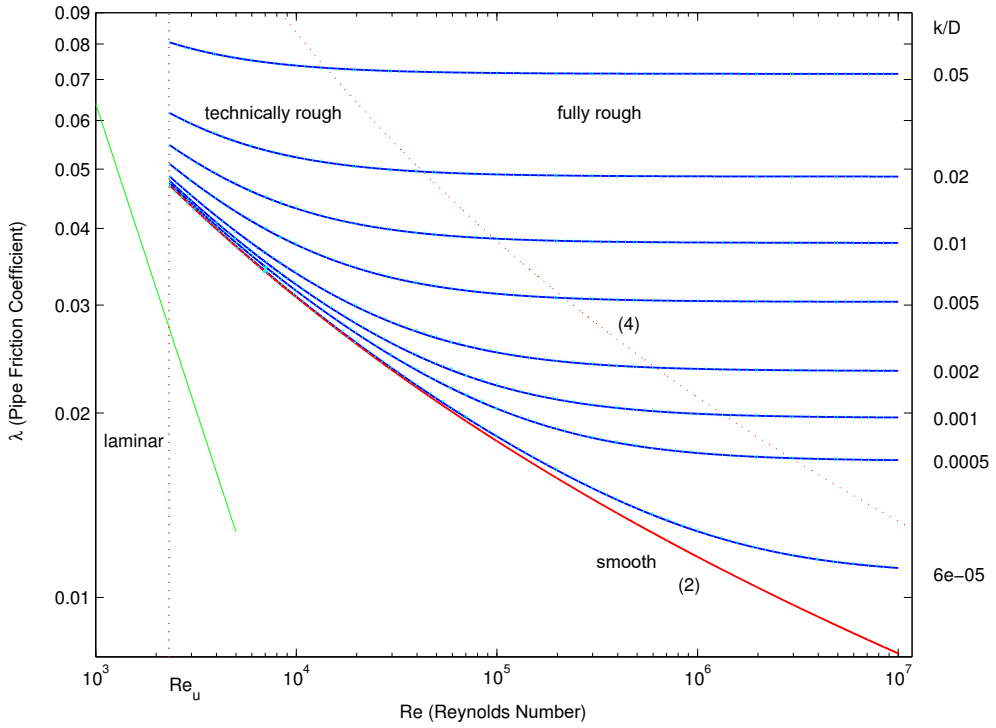

Figure 4: Moody diagram including Chen's formula

is an explicit formula that matches Colebrook's formula very well, see Figure 4. The values for λ from equation (13) are shown as light blue dotted lines.

Fully rough pipe: For a fully rough pipe, the pipe friction coefficient depends only on the relative roughness. For this regime, the following formula is used, named after Prandtl, Kármán and Nikuradze:

$$\lambda = \left[1.14 - 2\log_{10}\left(\frac{k}{D}\right)\right]^{-2}. \tag{14}$$

This explicit formula is obtained by taking the limit of $\mathrm{Re} \to \infty$ in equation (12). The border between technically and fully rough pipe is marked by (4) in the Moody diagram.

2.2.3 Explicit Formulas from Practice

Since implicit formulas for the calculation of the pipe friction coefficient were historically too elaborate, some simple explicit approximation formulas were established. In [37] a brief overview of approximate formulas from practice is given and partly their fields of application are described. In the Moody diagram in Figure 5 the different formulas are

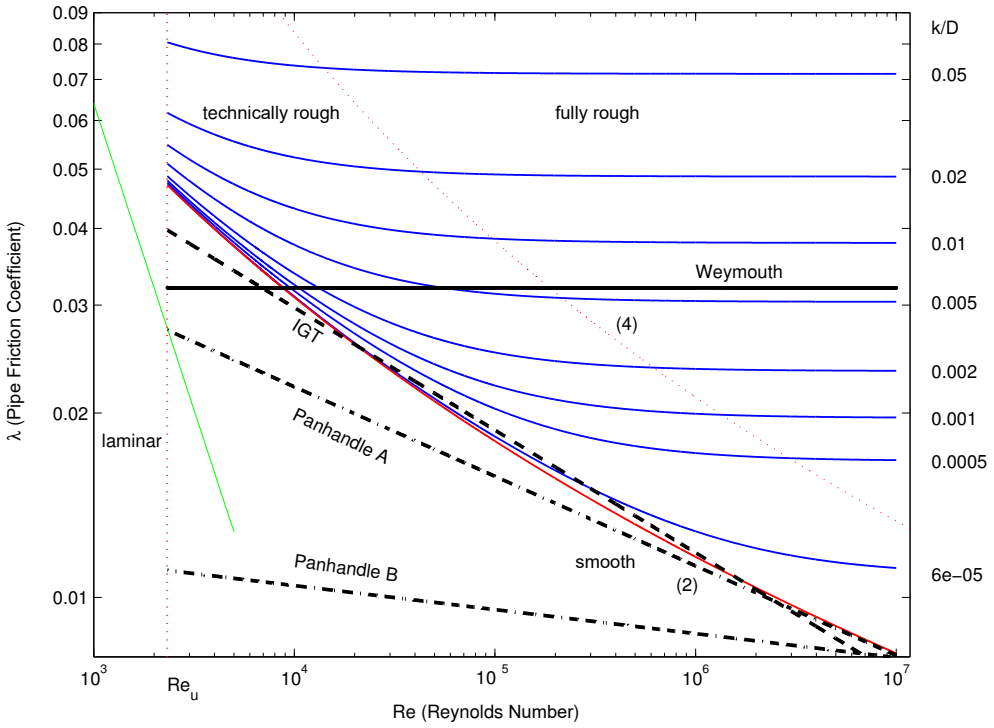

Figure 5: Moody diagram including formulas from practice

plotted (except the formula of Spitzglass, because here $D = 1\,\mathrm{m}$ was used, so that the formula of Spitzglass is not applicable).

Formula of Spitzglass (1912):

$$\lambda = \frac{4\left(1 + \frac{3.6}{D} + 0.03D\right)}{354}. \tag{15}$$

Only applicable for tubes with maximum diameter 10.95 in (27.8 cm) [37].

Weymouth (1912):

$$\lambda = \frac{4}{(11.18D^{1/6})^2}. \tag{16}$$

As can be seen in Figure 5, this equation is suitable for $k \approx 0.005$ in the fully rough regime.

Panhandle A:

$$\lambda = \frac{4}{(6.87\,\mathrm{Re}^{0.07305})^2}. \tag{17}$$

Application: small Reynolds numbers [37].

Panhandle B:

$$\lambda = \frac{4}{(16.49\,\mathrm{Re}^{0.01961})^2}. \tag{18}$$

Application: higher Reynolds numbers (than Panhandle A) [37].

Both curves (Panhandle A and B) are below the curve for a hydraulically smooth pipe in Figure 5.

IGT equation: (from Institute of Gas Technology)

$$\lambda = \frac{4}{\left(4.619\,\mathrm{Re}^{0.1}\right)^2}. \tag{19}$$

This equation is a relatively good approximation for hydraulically smooth pipes at Reynolds numbers between about 10^4 and 10^7 [37].

2.2.4 Summary

The model accepted in practice is that of Colebrook or Colebrook-White (12). This equation can be applied over the entire turbulent range. All other formulas (especially from section 2.2.3) are approximations applicable only in a relatively small range, see (5). In the double-logarithmic scale, the formulas are only tangents to Colebrook's model, and only for certain parameters. An exception to this is the explicit formula of Chen (13), which gives very good results over the entire turbulent range. Thus, in the turbulent regime, one of the two formulas, the "exact" implicit one of Colebrook-White or the explicit formula of Chen should be used.

3 Incompressible Navier-Stokes Equations

When studying phenomena on a pipe, the use of incompressible Navier-Stokes equations is often justified in practice. With a typical flow rate of $|v| \approx 10\,\mathrm{m\,s^{-1}}$ and $c \approx 340\,\mathrm{m\,s^{-1}}$, a reference Mach number of $M = |v|/c \approx 0.03$ is obtained. If we now consider the case $M \to 0$ for the three-dimensional Euler equations and assume that pressure changes have

no significant effect on the internal energy, then the addition of viscous terms in the limit case yields the system

$$\begin{aligned} \nabla \cdot v &= 0, \\ \frac{\partial}{\partial t} v + \nabla \cdot (v \otimes v) + \nabla p^\star &= \frac{1}{2} \nabla \cdot \left(\nu \left(\nabla v + \nabla v^T \right) \right) + f, \end{aligned} \tag{INS}$$

where f is a source term. Here $v = (v_1, v_2, v_3)$ is the velocity vector and $p^\star$ is the hydrodynamic pressure. The mean kinematic viscosity of natural gas being $\nu = 13.9 \times 10^{-6}\,\mathrm{m^2\,s^{-1}}$ is very low.

4 Model Hierarchy for Isothermal Euler Equations

In the isothermal case, we assume $T = T_0$, hence the energy equation is omitted. Thus, the compressibility factor is given as in (6). The isothermal Euler equations are given by

$$\begin{aligned} \frac{\partial \rho}{\partial t} + \frac{\partial}{\partial x}(\rho v) &= 0, \\ \frac{\partial}{\partial t}(\rho v) + \frac{\partial}{\partial x}(p + \rho v^2) &= -\frac{\lambda}{2D} \rho v |v| - g \rho \sin(\alpha), \end{aligned} \tag{ISO1}$$

together with the equation of state $p = R\rho T z(p)$ with $z(p) = 1 + \alpha p$ as above.

Here the eigenvalues of the Jacobian matrix of the flux function are $\lambda_1 = v - c$ and $\lambda_2 = v + c$. Thus, in the subsonic case ($|v| < c$) one always has a characteristic directed to the right and a characteristic directed to the left.

4.1 Semilinear Equations

If $z(p) = z_0$ is assumed to be constant, the result is a constant speed of sound $c = \sqrt{p/\rho}$. Then, the term in the spatial derivative of the momentum equation can be transformed into

$$p + \rho v^2 = p \left(1 + \frac{v^2}{c^2} \right). \tag{20}$$

For small flow rates $|v| \ll c$, Osiadacz [31] suggests to approximate the term in parentheses by 1. (Alternatively, one can assume that $\frac{\partial}{\partial x}(\rho v^2)$ is small and continue to calculate with nonconstant z-factor.) This eliminates the nonlinearity on the left-hand side and results in a semilinear model:

$$\begin{aligned} \frac{\partial \rho}{\partial t} + \frac{\partial}{\partial x}(\rho v) &= 0, \\ \frac{\partial}{\partial t}(\rho v) + \frac{\partial p}{\partial x} &= -\frac{\lambda}{2D} \rho v |v| - g \rho \sin(\alpha). \end{aligned} \tag{ISO2}$$

In this model, the eigenvalues of the Jacobian matrix of the flux function are $\lambda_1 = -c$ and $\lambda_2 = c$ (a negative and a positive characteristic).

Another possibility to derive semilinear equations is to study small perturbations on a fast time scale around a constant density and velocity zero [5, Section 3.2.2]. We set

$$\tau = \frac{t}{\varepsilon}, \quad \rho(x,t) = \rho_0 + \varepsilon^\beta \rho_1\left(x, \frac{t}{\varepsilon}\right), \quad v(x,t) = \varepsilon^{\beta-1} w\left(x, \frac{t}{\varepsilon}\right) \tag{21}$$

with a small $\varepsilon > 0$ and $\varepsilon^\beta := D/\lambda$. Then, we recover model (M1) from [5]:

$$\begin{aligned} \frac{\partial \rho_1}{\partial \tau} + \rho_0 \frac{\partial w}{\partial x} &= 0, \\ \frac{\partial w}{\partial \tau} + \frac{p'(\rho_0)}{\rho_0} \frac{\partial \rho_1}{\partial x} &= -\frac{w|w|}{2}, \end{aligned} \tag{ISO2F}$$

completed with the gas law $p(\rho) = \rho T_w z(\rho, T_w)$, where T_w is the wall temperature. Introducing $q_0 := \rho_0 w$ as a first order approximation around ρ_0 to the mass flow, we may write

$$\begin{aligned} \frac{\partial \rho_1}{\partial \tau} + \frac{\partial q_0}{\partial x} &= 0, \\ \frac{\partial q_0}{\partial \tau} + p'(\rho_0) \frac{\partial \rho_1}{\partial x} &= -\frac{q_0|q_0|}{2\rho_0}. \end{aligned} \tag{22}$$

This is a well-known model on the fast time scale.

If we follow the scaling approaches in [5] for the friction-dominant case, we obtain the model (FD1) (= friction dominated) presented there:

$$\begin{aligned} \frac{\partial \rho}{\partial t} + \frac{\partial}{\partial x}(\rho v) &= 0, \\ \frac{\partial p}{\partial x} &= -\frac{\lambda}{2D} \rho v |v| - g\rho \sin(\alpha), \end{aligned} \tag{ISO3}$$

where additionally the gravitational force was neglected in the asymptotic consideration. The parabolic character of the pressure can be made visible by equivalent transformations. With $\alpha = 0$ this results in (model (FD1b) from [5]):

$$\begin{aligned} \frac{\partial p}{\partial t} &= \frac{1}{2}\sqrt{\frac{DRTz_0}{\lambda}} \frac{\frac{\partial^2}{\partial x^2} p^2}{\sqrt{\left|\frac{\partial}{\partial x} p^2\right|}}, \\ \frac{\partial p}{\partial x} &= -\frac{\lambda}{2D} \rho v |v| . \end{aligned} \tag{ISO3P}$$

Typically, the pressure is then specified at both ends. These types of models are also discussed in the gas literature [31].

4.2 Algebraic Equations

In the stationary case the time derivatives disappear. Neglecting gravity and using a constant compressibility factor $z = z_0$, the equations are as follows:

$$\begin{aligned} \frac{\partial}{\partial x}(\rho v) &= 0, \\ \frac{\partial p}{\partial x} &= -\frac{\lambda}{2D}\rho v\,|v|\,. \end{aligned} \tag{ISO4}$$

The flux ρv is thus constant in space (and is given by the boundary condition) and the second equation can be solved analytically for p (transforming: $\rho v\,|v| = \frac{c^2 \rho v |\rho v|}{p}$):

$$p(x) = \sqrt{p_{in}^2 - \frac{\lambda c^2 x}{D}\rho v\,|\rho v|}$$

bzw.

$$p_{out} = \sqrt{p_{in}^2 - \frac{\lambda c^2 L}{D}\rho v\,|\rho v|}\,. \tag{ISO4-ALG}$$

Here L is the length of the pipe with coordinate $x \in [0, L]$ and p_{in} and p_{out} are the inlet and outlet pressure, respectively. If the flow is now represented by the pressure difference in this case, the so-called Weymouth equation is obtained by solving for ρv.

5 Model Hierarchy for Temperature-Dependent Euler Equations

For the temperature-dependent models, we want to proceed analogously to the isothermal models.

5.1 Simplified Nonlinear Equations

Starting from the full Euler equations (TA1), we first assume that for small velocities the temporal and spatial derivatives of ρv^2 and also ρv^3 are negligible. This results in the model

$$\begin{aligned} \frac{\partial \rho}{\partial t} + \frac{\partial}{\partial x}(\rho v) &= 0, \\ \frac{\partial}{\partial t}(\rho v) + \frac{\partial p}{\partial x} &= -\frac{\lambda}{2D}\rho v\,|v| - g\rho\sin(\alpha), \\ \frac{\partial}{\partial t}(\rho e) + \frac{\partial}{\partial x}(\rho v e + p v) &= -\frac{k_w}{D}(T - T_w)\,, \end{aligned} \tag{TA2}$$

together with the equation of state $p = R\rho T z(p,T)$. In contrast to the isothermal case, the equation remains nonlinear when these terms are omitted. The total energy E is now given only by $E = \rho e$ (compared to $E = \rho e + \frac{1}{2}\rho v^2$ for the full equations). Also, the equation of state continues to depend in a nonlinear way on p and T.

If we again follow the scaling approaches in [5] for the friction-dominant case, we obtain their model (ET3):

$$\begin{aligned} \frac{\partial \rho}{\partial t} + \frac{\partial}{\partial x}(\rho v) &= 0, \\ \frac{\partial p}{\partial x} &= -\frac{\lambda}{2D}\rho v\,|v| - g\rho\sin(\alpha), \\ \frac{\partial}{\partial t}(\rho e) + \frac{\partial}{\partial x}(\rho v e + p v) &= -\frac{k_w}{D}(T - T_w), \end{aligned} \tag{TA3}$$

where the gravitational influences were generally neglected in the asymptotic consideration.

To calculate the characteristics, the term $\varepsilon\frac{\partial}{\partial t}(\rho v)$ has to be added in the second equation. In the limit case $\varepsilon \to 0$ the eigenvalues $\lambda_1 \to -\infty$, $\lambda_2 = v$ and $\lambda_3 \to \infty$ are obtained, i.e. one characteristic depending on the flow direction and two characteristics with infinite propagation velocity.

5.2 Stationary Model

As with the isothermal models, a steady state can be assumed here as well. The resulting equations are (neglecting gravity):

$$\begin{aligned} \frac{\partial}{\partial x}(\rho v) &= 0, \\ \frac{\partial p}{\partial x} &= -\frac{\lambda}{2D}\rho v\,|v|, \\ \frac{\partial}{\partial x}(\rho v e + p v) &= -\frac{k_w}{D}(T - T_w), \end{aligned} \tag{TA4}$$

From the first equation it follows again that ρv is constant in space. However, since the more complex equation of state, with $z = z(p,T)$ nonlinear, applies here, the other two equations cannot directly be solved analytically. For this purpose, further simplifications may have to be assumed, such as a constant compressibility factor. If one assumes that the compressibility factor is constant, the speed of sound c is also constant and $c^2 = p/\rho$ holds. The energy equation can then be simplified using $e = c_v T$ to

$$\frac{\partial}{\partial x}\left(\rho v(c_v T + c^2)\right) = -\frac{k_w}{D}(T - T_w), \tag{23}$$

and since ρv is again constant in space,

$$\frac{\partial T}{\partial x} = -\frac{k_w}{D c_v \rho v}\left(T - T_w\right). \tag{24}$$

The complete equations are thus given by

$$\begin{aligned} \frac{\partial}{\partial x}(\rho v) &= 0, \\ \frac{\partial p}{\partial x} &= -\frac{\lambda c^2}{2Dp}\rho v\left|\rho v\right|, \\ \frac{\partial T}{\partial x} &= -\frac{k_w}{D c_v \rho v}\left(T - T_w\right). \end{aligned} \tag{TA4b}$$

The exact solution of the energy equation is

$$T(x) = \left(T(x_0) - T_w\right) \cdot e^{-\frac{k_w}{D c_v \rho v}(x - x_0)} + T_w, \tag{25}$$

and the overall system reads (with $x_0 = 0$ and $x = L$)

$$\begin{aligned} \rho v &= \text{const.}, \\ p_{out} &= \sqrt{p_{in}^2 - \frac{\lambda c^2 L}{D}\rho v\left|\rho v\right|}, \\ T_{out} &= \left(T_{in} - T_w\right) \cdot e^{-\frac{k_w}{D c_v \rho v} L} + T_w. \end{aligned} \tag{TA4-ALG}$$

6 Model Hierarchy for Pipe Modeling

The models presented here differ in each case by omitting individual terms or applying scaling arguments from [5]. In addition, simplified equations of state may be assumed. Figures 6 and 7 give a brief summary of the simplification steps.

7 Net Modeling

Let $G = (\mathcal{V}, \mathcal{E})$ be the graph of the gas net with the nodes $\mathcal{V} = \{v_1, n_2, \ldots, v_V\}$ and the edges $\mathcal{E} = \{e_1, e_2, \ldots, e_E\}$ where $V = |\mathcal{V}|$ and $E = |\mathcal{E}|$. For a unique description of the network equations, we give each edge a fixed orientation, see Figure 8. Correspondingly, we denote the two nodes belonging to an edge as left node v_L and as right node v_R with the convention that the edge is always oriented from the left to the right node. We consciously avoid the notation v_{in} and v_{out} since the flow direction can change during the network operation. Positive flow values correspond to flows from the left to the right node. Negative flow values mean flows from right to left node.

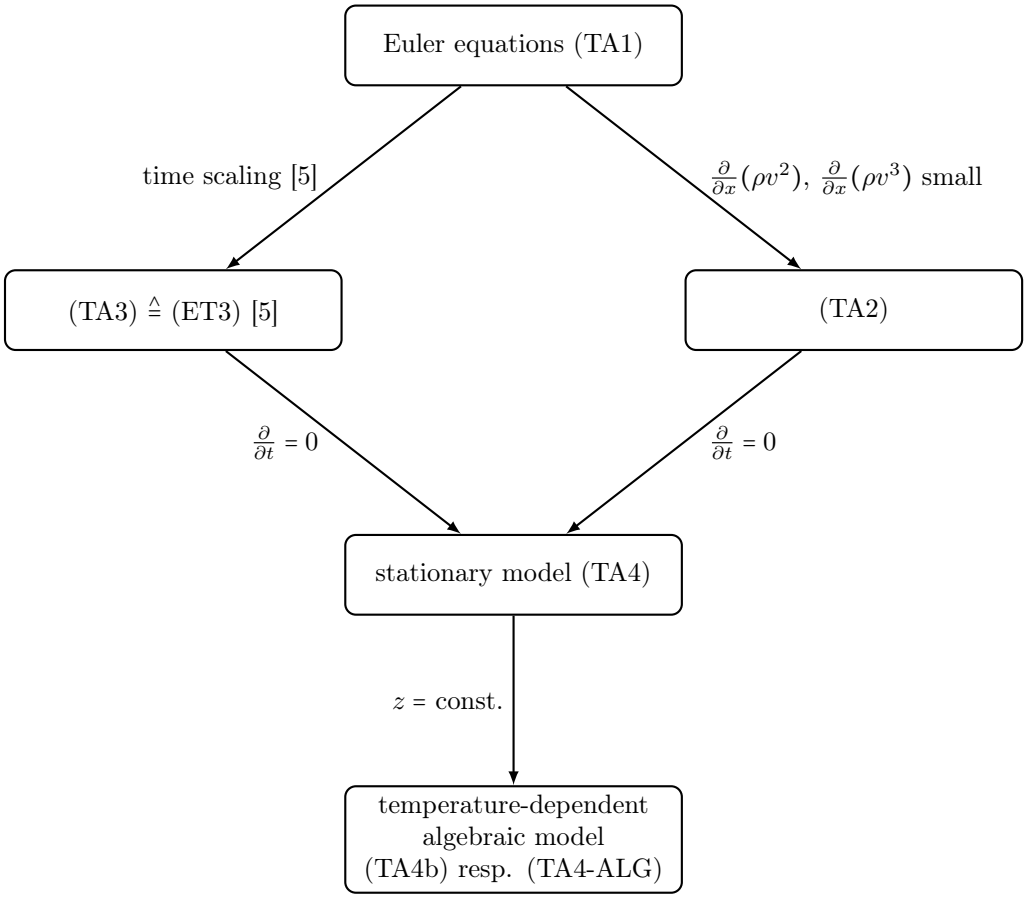

Figure 6: Model hierarchy for the temperature-dependent Euler equations

7.1 Incidence Matrices

The assignment of the left and right nodes of an edge to the nodes $\mathcal{V}$ can be easily described by the incidence matrices A_L, $A_R \in \mathbb{R}^{V \times E}$ defined as follows.

$$(A_L)_{ij} = \begin{cases} -1, & \text{if node } v_i \text{ is the left node of the edge } e_j, \\ 0, & \text{else,} \end{cases}$$

$$(A_R)_{ij} = \begin{cases} +1, & \text{if node } v_i \text{ is the right node of the edge } e_j, \\ 0, & \text{else.} \end{cases}$$

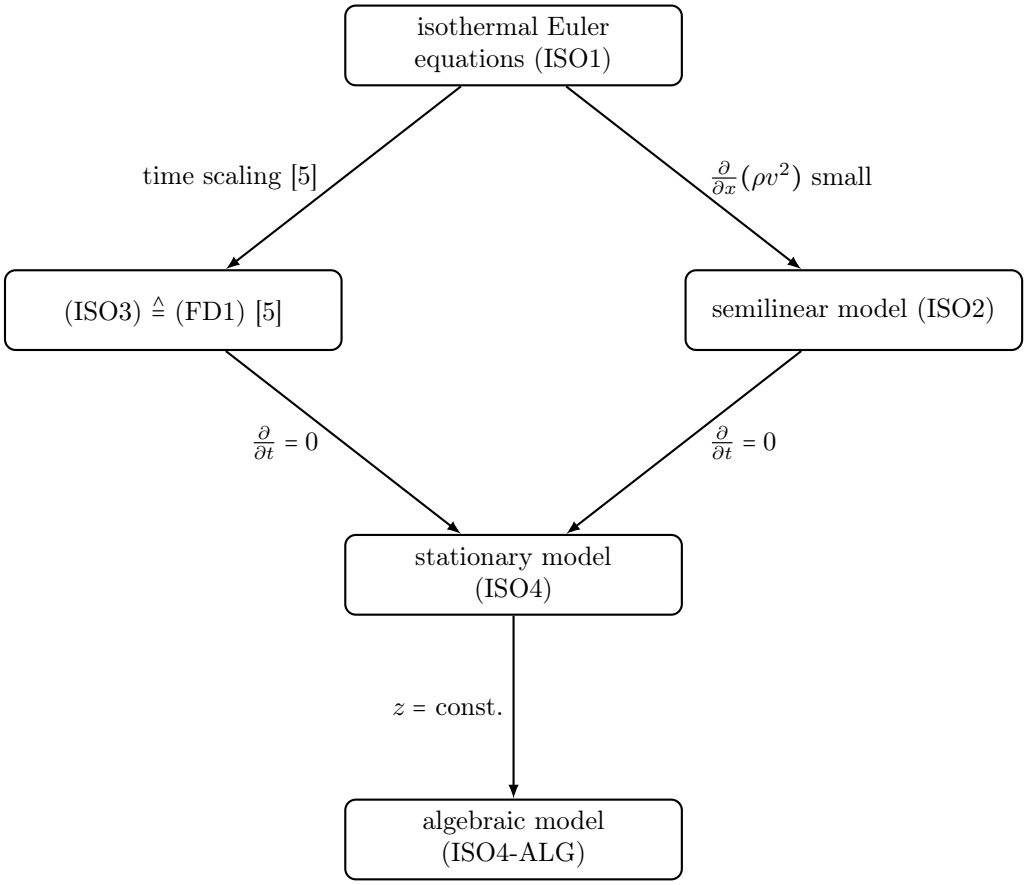

Figure 7: Model hierarchy for the isothermal Euler equations

We assume that there are no edges whose left and right nodes are identical, i.e. we do not allow *self-loops*. Then it follows for the incidence matrix $A := A_L + A_R$ that

$$(A)_{ij} = \begin{cases} -1, & \text{if node } v_i \text{ is the left node of the edge } e_j, \\ +1, & \text{if node } v_i \text{ is the right node of the edge } e_j, \\ 0, & \text{else.} \end{cases}$$

7.2 Flow Balance Equations

Using the incidence matrices it is easy to formulate the flow balance equations for each node. Let the i-the component of q_L be the flow of the edge e_i on the left side and the i-th component of q_R be the flow of the edge e_i at the right side, see Figure 8. Then, the flow balance equations are given by

$$A_L q_L + A_R q_R = 0. \tag{26}$$

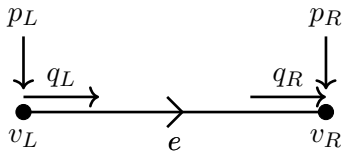

Figure 8: Branch flows q_L and q_R as well as pressures p_L and p_R at the left and right nodes of an oriented edge e

The i-th row of the equations system (26) reflects the sum of all incoming flows (with minus sign) and outgoing flows (with plus sign) at the node v_i.

For a simple modeling of supply and demand flows, we use the model of supply and demand nodes. Correspondingly, we can write the flow balance equations as

$$A_L q_L + A_R q_R = q_s \tag{27}$$

where q_s denotes the amount of supplied gas (with plus sign) and extracted gas (with minus sign) at the network nodes. If a node is neither a supply nor a demand node then the corresponding component of q_s is zero. For the special case that all flows on the edges are constant (i.e. independent from the position) then we have $q_L = q_R =: q$ and the flow balance equations read

$$Aq = q_s. \tag{28}$$

7.3 Pressure Differences

The operation of network elements often depends on the pressure difference between two nodes. The incidence matrices can be used to easily describe these pressure differences. First, we can express the vector p_L of all left pressures and the vector p_R of all right pressures belonging to the edges (see Figure 8)

$$p_R = A_R^\top p \quad \text{und} \quad p_L = -A_L^\top p. \tag{29}$$

where p is the vector of all node pressures. Thus, the pressure differences along all edges are given by

$$p_R - p_L = A_R^\top p + A_L^\top p = A^\top p. \tag{30}$$

7.4 Network Elements

The next subsections describe the element equations for typical gas network elements. Note that we introduced p_L, p_R, q_L and q_R as vectors of pressures and flows of all edges of the network. In the following subsections, they are used for the pressures and flows of the described elements only.

7.4.1 Pipes

The pipe modeling is described in detail on different modeling levels in Section 2. For an overview see Section 6.

7.4.2 Valves

Valves are available in various designs and model formulations. The easiest modeling describes a valve as a switch with two states *open* and *closed*. In the *open* state we have

$$q := q_R = q_L, \quad p_L = p_R. \tag{31}$$

In the *closed* state there is no flow, i.e.

$$q := q_R = q_L = 0. \tag{32}$$

7.4.3 Check Valve

Check valves are self controlling valves that allow only one flow direction. They are used to protect the network against pressure overload and loss of outflow in the event of pipe breaks [4]. We choose the pipe orientation such that it directs along the allowed flow direction. Again we have to states: open and closed. If the check valve is *open* we have

$$q := q_R = q_L, \quad p_L = p_R. \tag{33}$$

Analogously, we obtain for *closed* check valves

$$q := q_R = q_L = 0. \tag{34}$$

The control of the check valves can be modeled as follows:

1. If the valve is closed and $p_L > p_R$ then the valve turns to open state.
2. If the valve is open and $q_R < 0$ then the valve turns to closed state.

7.4.4 Resistances

A resistance is a simple edge element to describe the hydraulic resistance of a device. It is also used model the pressure loss in network components as for example filter systems. The pressure loss $\Delta p = p_L - p_R$ can be modeled by (see [14, 36])

$$p_L - p_R = \frac{\zeta}{2}\rho_L v|v| = \frac{\zeta}{2}\frac{q|q|}{\rho_L A^2} \tag{35}$$

with $q := q_L = q_R$. Here, ζ, v, ρ_L and A are the pressure loss coefficient, the velocity of the gas the gas density at the left node (= inflow node) and the pipe cross-section. If the

real gas factor z_0 is assumed to be constant then we have $p_L = \rho_L c^2$ with the constant speed c of sound. Hence,

$$p_L(p_L - p_R) = bq|q| \tag{36}$$

with $b := \frac{c^2}{2a^2}\zeta$. If the pressure loss coefficient and/or the pipe cross-section are not known then the pressure loss is modeled as constant (see [36]):

$$p_L(p_L - p_R) = \operatorname{sign}(q)\xi \tag{37}$$

with a pressure loss constant ξ.

7.4.5 Controllers with Characteristic Curves

Controller control the flow in dependence on the adjacent pressures and a proportional opening parameter o, i.e.,

$$q := q_R = q_L = f(p_L, p_R, o) \tag{38}$$

where f is describes the characteristic curve. One example is the characteristic curve for Mokveld valves (see [17]):

$$q := q_R = q_L = c_1(o)\frac{241 c_2 p_L(p_* - 0.148 p_*^3)}{\sqrt{\rho T z}}, \quad p_* = \min\left\{1.5,\ \frac{1.63}{c_2(o)}\sqrt{\frac{p_L - p_R}{p_L}}\right\} \tag{39}$$

where the coefficients $c_1(o)$ and $c_2(o)$ depend on the parameter o.

7.4.6 Preheater

The high pressure is reduced at the take-off stations. Gas preheating is required to prevent impermissible cooling when reducing the pressure (due to the Joule-Thomson effect). The gas is heated in heat transfer stations so far that the gas temperature is higher than the dew point of the gas after throttling [4]. The temperature difference depends on the pressure difference and can be described by [36]

$$\frac{\mathrm{d}T}{\mathrm{d}p} = \mu_{JT}(p,T) = \frac{R}{\tilde{c}_p}\frac{T^2}{p}\frac{\partial z(p,T)}{\partial T}. \tag{40}$$

Here, μ_{JT} is the Joule-Thomson coefficient, R is the universal gas constant, $\tilde{c}_p$ is the molar heat capacity and $z(p,T)$ is the real gas factor. The simple approximation by one implicit Euler discretization step is usually sufficient as model for simulation and optimization [36]. Then, we obtain

$$\frac{T_R - T_L}{p_R - p_L} = \mu_{JT}(p_R, T_R) = \frac{R}{\tilde{c}_p}\frac{T_R^2}{p_R}\frac{\partial z}{\partial T}(p_R, T_R), \tag{41}$$

as element equation for the preheater. There, T_L and T_R are the temperatures at left and right node of the preheater. Correspondingly, T_L is the gas temperature before the heating and T_R is the gas temperature after the heating. The flow value keeps constant during the heating, i.e., $q = q_L = q_R$.

7.4.7 Compressor

Compressors are required in gas pipelines since the pressure decreases significantly after approx. 100 to 150 km and the gas flows more slowly due to the friction of the gas flow on the pipe walls. The compression costs depend on the number of compressors and the compression ratio. Low compression ratios result in lower energy costs but require more compressor stations [4]. After compression, the pressure within a gas pipeline is up to 100 bar [23]. The compression is usually described by compressor maps (see Figure 9) derived from measured values of the enthalpy H_{ad}, i.e., the energy needed to compress one unit of mass of the gas.

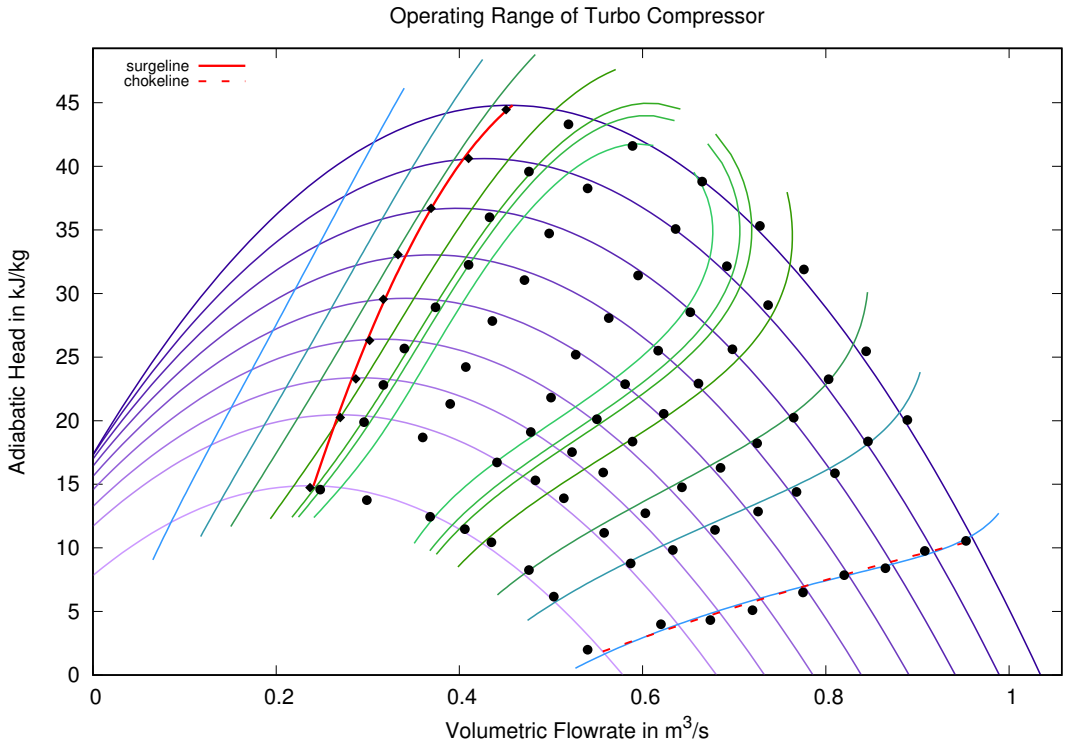

Figure 9: Compressor map of a turbo compressor: Isentropic enthalpy change H_{ad} vs. volume flow $Q = q/\rho$. The horizontal isolines describe the characteristic curves with constant speed, i.e., with constant drive. The vertical isolines represent the characteristic curves with constant efficiency η_{ad}.

It must be ensured that compressors do not operate outside the stability limits of the map. Otherwise the stress would be too high for the machine and its function could be

destroyed. The enthalpy change H_{ad} depends on the pressure and the temperature and can be described as [6]

$$H_{ad} = z(p_L, T_L) T_L R_s \frac{\kappa}{\kappa - 1} \left(\left(\frac{p_R}{p_L} \right)^{\frac{\kappa-1}{\kappa}} - 1 \right) \tag{42}$$

where the isentropic exponent κ depends on pressure and temperature. However, it is often considered as constant $\kappa = 1.29$ in practice [28]. Furthermore, R_s is the specific gas constant and T_L is the temperature at the inflow of the compressor. Correspondingly, p_L and p_R are the pressures at the inflow and outflow of the compressor. The temperature T_R at the outflow is given by [6]:

$$T_R = T_L \left(\frac{p_R}{p_L} \right)^{\frac{\kappa-1}{\kappa}} . \tag{43}$$

Combining (42) and the compressor map, the relationship between pressure and flow of a compressor is given.

For turbo compressors, the compressor map is typically used for quadratic approximations for the lower, left, upper and right boundary of the compressor map. This gives rise to the conditions

$$\begin{aligned} H_{ad} &\geq \alpha_2^i Q^2 + \alpha_1^i Q + \alpha_0^i \quad i = 1, 2, \\ H_{ad} &\leq \alpha_2^i Q^2 + \alpha_1^i Q + \alpha_0^i \quad i = 3, 4. \end{aligned} \tag{44}$$

Beside turbo compressors also reciprocating compressors are used [34]. Reciprocating compressors are usually used only for small compressor capacities. For higher compressor capacities, one uses mainly turbo compressors with gas turbine drive [6].

7.4.8 Cooler

The compression of the gas leads to a temperature increase due to the Joule-Thomson effect. Therefore gas coolers are used for regulated cooling of the gas within compressor stations. The temperature decrease can be modeled as [28]

$$T_R = T_c + (T_L - T_c) \exp\left(-\frac{k}{q} \right), \tag{45}$$

with $q = q_L = q_R$. Again, T_L and T_R are the temperature at the inflow and the outflow of the cooler. T_c is the temperature of the coolant at the inflow and k is a constant.

7.4.9 Compressor Groups and Compressor Stations

Typical real gas networks contain compressor stations with multiple compressors. An important special case are simple compressor stations that compress gas along one pipeline

in a fixed direction. Common simulation software such as SIMONE [26] provides macro elements describing simple compressor stations. In accordance to the terminology from the ForNe project [34] we denote them as *compressor groups*.

A compressor group consists of a number of compressors, one upstream and one downstream resistor modeling the cumulative pressure loss in the pipes within the compressor station, a cooler to prevent overheating and a so-called *bypass*, which controls the flow of the gas via a valve without compression, see Figure 10. A compressor group allows a number of *configurations*, whereby a configuration specifies how a subset of the compressors is switched. There are series connections of parallel connections of compressors possible. Each compressor within one configuration is used at most once. Within the network, a compressor group is modeled by an edge connecting a node v_L with a node v_R. In the active case (no bypass mode), the compression direction points from v_L to v_R.

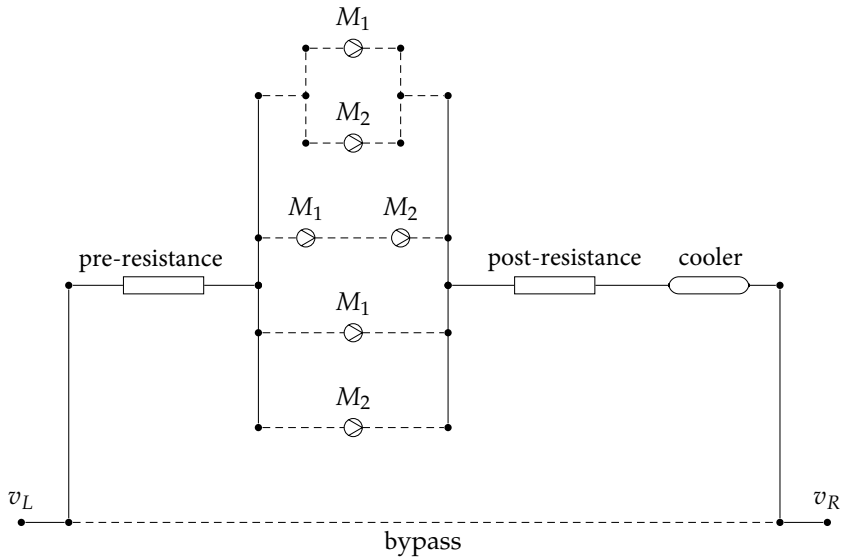

Figure 10: Schematic representation of a compressor group with two compressors, all theoretically possible configurations of these compressors and the bypass mode [34]. Depending on the selected configuration, gas flows through exactly one of the dotted paths, i.e., either via the bypass without pressure loss or via one compressor configuration, whereby the pressure loss in internal pipe connections is modeled by additional resistances.

In complex gas networks, *compressor stations* connect several pipelines with each other. They are used to distribute gas between these pipelines, see Figure 11. A compressor station can be operated in different *routes*. A route defines how the gas flows through the compressor station and which compressors are active. The possible routes are usually modeled over larger subnetworks that contain valves beside pipes, compressors and compressor groups [34].

Suitable switching configurations for the valves and compressors can then be used to

model the possible routes in the real network. Each route corresponds to a fixed state of each valve (open or closed) and each compressor (open, active, bypass) of the sub-network. For an overview of further and especially simplified models for compressors and compressor stations we refer to [16].

7.5 Classes of Network Models

This section provides a list of sample model classes for real gas networks. We start with the simplest one describing networks with pipes only and using the pure algebraic ISO4 modeling for pipes. It neglects valves and compressors that belong to all real gas transport networks (over long distances) but allows a fast and rough approximation of the flow through the pipe network.

Beside the description of the gas network elements we have to consider the flow balance equation and the fact that the pressure at each end of a branch element (pipe, valve, resistor, compressor or compressor group) equals the pressure at the node connected to the end. Therefore, we use the pipe equations using pressure p and mass flow q instead of density ρ and velocity v. For that we exploit the state equation

$$p = R\rho T z(p)$$

and the 1D representation of mass flow

$$q = \frac{\partial m}{\partial t} = \rho \frac{\partial V}{\partial t} = \rho a v$$

with m being the mass, V being the volume and a being the cross-section of the pipe. In contrast to the literature we use a lowercase letter a instead of A in order to avoid misunderstandings with the incidence matrix A. Both equations yield

$$\rho = \frac{p}{RTz(p)}, \quad \rho v = \frac{q}{a}, \quad v = \frac{RT}{a}\frac{z(p)}{p} q. \tag{46}$$

7.5.1 Pipe Network with ISO4 Modeling

Regarding (46), the stationary pipe equations (ISO4) are given by

$$\begin{aligned} \partial_x q &= 0, \\ \partial_x (p^2) = 2p\partial_x p &= -\frac{c^2 \lambda}{a^2 D} q\,|q| \end{aligned} \tag{47}$$

with the sound velocity c satisfying $c^2 = RTz_0$ for $z(p) \equiv z_0$. We see that q is constant with respect to space on each pipe and the second equation yields

$$p^2(x_R) - p^2(x_L) = -\frac{c^2 \lambda}{a^2 D} q\,|q|\,(x_R - x_L) \tag{48}$$

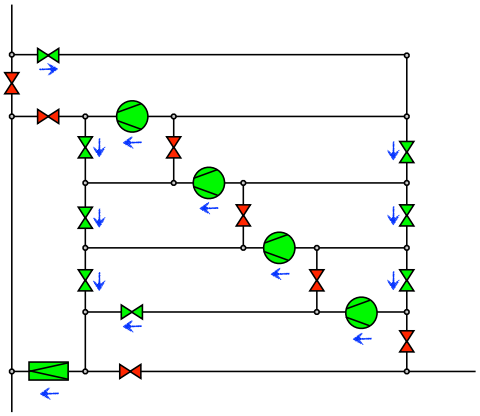

(a) 4-fold parallel compressed gas flow from north to south

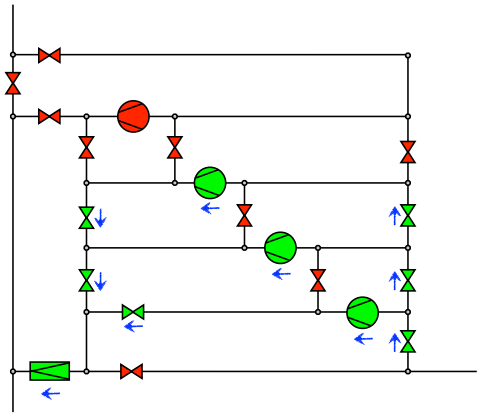

(b) 3-fold parallel compressed gas flow from east to south

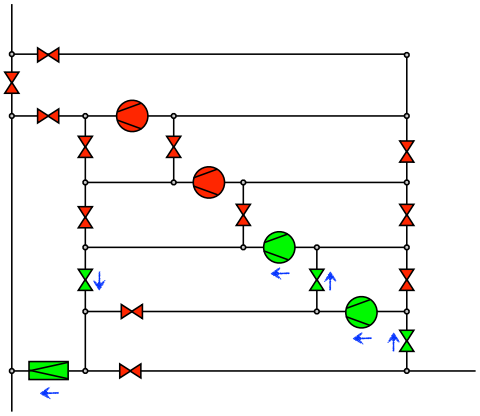

(c) 2-fold serial compressed gas flow from east to south

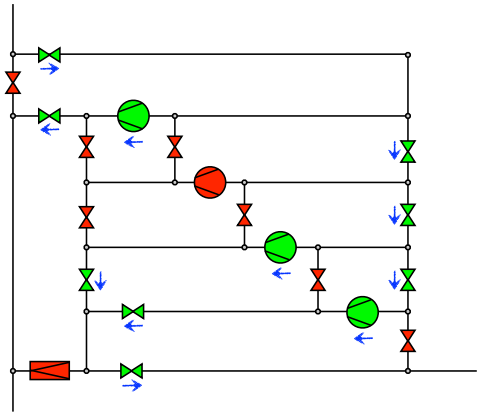

(d) 2-fold parallel compressed gas flow from north to east and 1-fold compressed gas flow from north to south

Figure 11: Four routes of a real compressor station that connects one north to south pipeline with a pipeline directing to east in a T-shaped form.

with the end points x_L and x_R of the pipe. Regarding the flow balance equation (28), the whole network system is then given by

$$\begin{aligned} (A_R^\top p)^2 - (A_L^\top p)^2 &= f(q), \\ Aq &= q_s \end{aligned} \tag{PNET-ISO4}$$

with the vector of nodal pressures $p = (p_1, \dots, p_V)^\top$, the vector of pipe flows $q = (q_1, \dots, q_E)^\top$ and

$$f(q) = \begin{pmatrix} \vdots \\ -\frac{c_j^2 \lambda}{a_j^2 D_j} q_j |q_j| (x_{R_j} - x_{L_j}) \\ \vdots \end{pmatrix}$$

7.5.2 Pipe Network with ISO2 Modeling

Regarding (46), the pipe equations (ISO2) are represented by

$$\begin{aligned} \partial_t \left(\frac{p}{z(p)} \right) + \frac{RT}{a} \partial_x q &= 0, \\ \partial_t q + a \partial_x p &= -\frac{\lambda RT}{2aD} \frac{z(p)}{p} q |q| - \frac{ag}{RT} \frac{p}{z(p)} \sin(\alpha). \end{aligned} \tag{49}$$

Due to the flow balance equation (28), the whole pipe network is given by

$$\begin{aligned} \partial_t g(p) + D_q \partial_x q = 0, \quad \partial_t q + D_p \partial_x p &= f(p,q), \\ p(x_L, \cdot) = -A_L^\top \bar{p}, \quad p(x_R, \cdot) &= A_R^\top \bar{p}, \\ q(x_L, \cdot) = q_L, \qquad q(x_R, \cdot) &= q_R, \\ A_L q_L + A_R q_R &= q_s, \end{aligned} \tag{PNET-ISO2}$$

with the vector of nodal pressures $\bar{p} = (\bar{p}_1, \dots, \bar{p}_V)^\top$, the vector of pipe pressures $p = (p_1, \dots, p_E)^\top$, the vector of pipe flows $q = (q_1, \dots, q_E)^\top$,

$$D_q = \operatorname{diag}\{\dots, \tfrac{R_j T_j}{a_j}, \dots\}, \qquad D_p = \operatorname{diag}\{\dots, a_j, \dots\}$$

and

$$g(p) = \begin{pmatrix} \vdots \\ \frac{p}{z(p)} \\ \vdots \end{pmatrix}, \qquad f(p,q) = \begin{pmatrix} \vdots \\ -\frac{\lambda R_j T_j}{2aD} \frac{z(p_j)}{p_j} q_j |q_j| - \frac{a_j g}{R_j T_j} \frac{p_j}{z(p_j)} \sin(\alpha_j) \\ \vdots \end{pmatrix}.$$

Notice that x_L and x_R are also considered as vector of all left and right end points here. One can apply various discretization approaches in space and time to the network

equation system (PNET-ISO2) for stable simulation and efficient optimization. One opportunity is the implicit box scheme [21, 22]. Using a two-point discretization yields

$$\begin{aligned}
\frac{1}{2}\left(g(-A_L^\top \bar{p}^{n+1}) + g(A_R^\top \bar{p}^{n+1})\right) &= \frac{1}{2}\left(g(-A_L^\top \bar{p}^{n}) + g(A_R^\top \bar{p}^{n})\right) - \Delta t\, \tilde{D}_q \cdot \left(q_R^{n+1} - q_L^{n+1}\right), \\
\frac{1}{2}\left(q_L^{n+1} + q_R^{n+1}\right) &= \frac{1}{2}\left(q_L^{n} + q_R^{n}\right) - \Delta t\, \tilde{D}_p \cdot \left(A_R^\top \bar{p}^{n+1} + A_L^\top \bar{p}^{n+1}\right) \\
&\quad + \frac{1}{2}\Delta t\left(f(-A_L^\top \bar{p}^{n+1}, q_L^{n+1}) + f(A_R^\top \bar{p}^{n+1}, q_R^{n+1})\right), \\
A_L q_L + A_R q_R &= q_s
\end{aligned} \tag{PNET-ISO2-IBOX}$$

with

$$\tilde{D}_q = \operatorname{diag}\{\ldots, \tfrac{R_j T_j}{a_j (x_{R_j} - x_{L_j})}, \ldots\}, \qquad \tilde{D}_p = \operatorname{diag}\{\ldots, \tfrac{a_j}{x_{R_j} - x_{L_j}}, \ldots\}.$$

The upper index n denotes the n-th time step with stepsize Δt. This nonlinear method was already applied successfully in connection with a piecewise linearization [10]. It is suitable for stiff as well as for non-stiff source terms. The time stepsize is only weakly limited by a lower boundary $\Delta t \geq \frac{\Delta x}{2c}$ if $z(p) \equiv z_0$, see [21, 22]. We refer here also to other classical finite volume methods as the Lax-Friedrichs, the vector splitting or the Godunov method [24]. Such discretizations require equation dependent considerations for the combined realization of boundary and coupling conditions as well as the use of limiter approaches. It leads to a significantly more complex structure and the well-known CFL condition (CFL = Courant-Friedrichs-Levy) that is given as $c\Delta t \leq \Delta x$ for the (ISO2) model with $z(p) \equiv z_0$.

In order to handle a possible stiffness of the friction term (and hence more restrictive limits to the time stepsize), so-called IMEX-Runge-Kutta methods have proven their value in practice [19]. There, the hyperbolic part is treated explicitly and the reaction part is treated implicitly. In context of differential-algebraic equations arising from semi-dscretizations in space implicit as well as semi-explicit methods are common [1].

A stable discretization without a time stepsize limit can be obtained when the spatial discretization is adapted to the network topology, namely to the topological connection of supply and demand nodes, and an A-stable time-step method is applied to the resulting differential-algebraic system of index 1, see [3, 18].

7.5.3 Pipe Networks with Valves

In case of pipe networks with valves we have additional valve flows q^v. For pipes modeled by ISO4 we obtain the following extension of the system (PNET-ISO4):

$$\begin{aligned}
(A_R^\top p)^2 - (A_L^\top p)^2 &= f(q), \\
S(A_{v_R}^\top p - A_{v_L}^\top p) + (I - S) q_v &= 0, \\
Aq + A_v q_v &= q_s.
\end{aligned} \tag{PVNET-ISO4}$$

with $S = \mathrm{diag}\{\ldots, s_j, \ldots\}$. Here, $A = A_L + A_R$ and $A_v = A_{v_L} + A_{v_R}$ are the incidence matrices for pipes and valves, respectively. The switching parameter s_j describes the open/closed state of the valve with number j: In open state we have $s_j = 1$, in closed state $s_j = 0$. In case of other valve models (check valves for example), one has to adapt the valve equations appropriately.

In case of an (ISO2) modeling for pipes we obtain the extension of system (PNET-ISO2):

$$\begin{aligned}
\partial_t g(p) + D_q \partial_x q = 0, \quad \partial_t q + D_p \partial_x p = f(p,q),\\
p(x_L,\cdot) = -A_L^\top \bar{p}, \quad p(x_R,\cdot) = A_R^\top \bar{p},\\
q(x_L,\cdot) = q_L, \qquad q(x_R,\cdot) = q_R,\\
S(A_{v_L}^\top \bar{p} - A_{v_R}^\top \bar{p}) + (I-S)q_v = 0,\\
A_L q_L + A_R q_R + A_v q_v = q_s.
\end{aligned} \tag{PVNET-ISO2}$$

7.5.4 Pipe Networks with Valves, Resistances, Coolers and Compressor Stations

As described before, real gas networks consist of pipes, valves, resistances, coolers and compressor stations. Correspondingly, we obtain (in case of ISO4 pipe modeling) the equation system

$$\begin{aligned}
Aq + A_v q_v + A_r q_r + A_l q_l + A_c q_c = q_s,\\
(A_R^\top p)^2 - (A_L^\top p)^2 = f(q),\\
S(A_{v_L}^\top p - A_{v_R}^\top p) + (I-S)q_v = 0,\\
f_r(A_{r_L}^\top p, A_{r_R}^\top p, q_r) = 0,\\
f_l(A_{l_L}^\top T, A_{l_R}^\top T, q_l) = 0,\\
H(q_c,u) - d\left(A_{c_L}^\top p, A_{c_R}^\top p, A_{c_L}^\top T\right) = 0,\\
f_c(A_{c_L}^\top p, A_{c_R}^\top p, A_{c_L}^\top T, A_{c_R}^\top T) = 0,\\
\text{+ conditions for routes for compressor stations}
\end{aligned} \tag{PVCNET-ISO4}$$

with

$$f_r(p_L, p_R, q) = \begin{pmatrix} \vdots \\ p_{Lj}(p_{Rj} - p_{Lj}) - b_j q_j |q_j| \\ \vdots \end{pmatrix},$$

$$f_l(T_L, T_R, q) = \begin{pmatrix} \vdots \\ T_{R_j} - T_{c_j} - (T_{L_j} - T_{c_j}) \exp\left(-\frac{k_j}{q_j}\right) \\ \vdots \end{pmatrix},$$

$$f_c(p_L, p_R, T_L, T_R) = \begin{pmatrix} \vdots \\ T_{R_j} - T_{L_j} \left(\frac{p_{R_j}}{p_{L_j}}\right)^{\frac{\kappa-1}{\kappa}} \\ \vdots \end{pmatrix}, \qquad H(q, u) = \begin{pmatrix} \vdots \\ H_j(q_j, u_j) \\ \vdots \end{pmatrix},$$

$$d(p_L, p_R, T) = \begin{pmatrix} \vdots \\ z(p_{L_j}, T_j) T_j R_s \frac{\kappa}{\kappa-1} \left(\left(\frac{p_{R_j}}{p_{L_j}}\right)^{\frac{\kappa-1}{\kappa}} - 1 \right) \\ \vdots \end{pmatrix}.$$

Here, A, A^v, $A^r = A^r_L + A^r_R$, $A^l = A^l_L + A^l_R$ and $A^c = A^c_L + A^c_R$ are the incidence matrices for the pipes, valves, resistances, coolers and compressors. T represents the vector of temperatures at the nodes. T_{c_j} is the temperature of the coolant in cooler with number j. Further, $H_j(q, u)$ is the flow-enthalpy characteristic curve of the compressor with number j depending on the control u. For compressor groups, one uses subnets as given in Figure 10. Then, (PVCNET-ISO4) can applied as for a set of single compressors.

8 Discretizations

In the following, we present a brief summary of basic numerical methods and concepts for the treatment of hyperbolic balance laws. These have to be supplemented by appropriate discretizations of boundary and coupling conditions as well as further network components like compressors and valves.

The Euler equations (TA1) on a single pipe can be formalized into a system of nonlinear balance equations of the form

$$\partial_t \mathbf{u} + \partial_x \mathbf{f}(\mathbf{u}) = \mathbf{g}(x, \mathbf{u}). \tag{50}$$

The standard method for solving these equations is the *finite volume method*. This method is based on the integral form of the equations above, which are often closer to the physics of the problem. This offers elegant ways to numerically solve even non-smooth physical phenomena such as shock waves, contact discontinuities and rarefaction waves at high precision. Among the best known classical methods are the Lax-Friedrichs and Godunov methods. The latter uses the solution of local Riemann problems at cell

boundaries, which is often replaced in practice by suitable approximations. The Lax-Friedrichs method, like other finite volume methods, can be regarded as a conservative *finite difference method*.

A common strategy is the coupling of high accuracy methods in regions with smooth solutions and TVD or TVB methods (total variation diminishing, total variation bounded) of lower order in regions with discontinuities. In between, flux and slope limiters mediate, as for example in MUSCL methods (monotonic upstream-centered scheme for conservation laws). An excellent summary can be found in the book by LeVeque [24]. Generalizations of the polynomial reconstructions of solutions across multiple cells used in these methods lead to the class of ENO and WENO methods (essentially non-oscillatory, weighted essentially non-oscillatory). An overview with further references can be found in the monograph by Shu [38]. Solving Riemann problems, especially at junctions in networks, can become very costly and also prevents a compact notation of a discretization to be used in optimization. Central methods, originating from work by Nessyahu and Tadmor [30] that use staggered grids, avoid this difficulty and are easy to implement, especially in 1D. Among this class are the attractive box methods introduced by Wendroff [41]. In time, both explicit - which have to satisfy a Courant-Friedrichs-Levy (CFL) condition of the form $\triangle t \leq c(\mathbf{u}) \triangle x$ for stability reasons - and implicit methods are used. IMEX-Runge-Kutta methods allow an explicit discretization of the hyperbolic part and an implicit discretization of the source $\mathbf{g}(x, \mathbf{u})$. Also very popular are SSP-Runge-Kutta and SSP multi-step (SSP = strong stability preserving) methods [19].

In contrast to finite volume methods, *Discontinuous Galerkin methods* (DG) [9] do not require reconstructions, since a higher order polynomial is already used in each cell. However, this also requires multiple degrees of freedom to be stored and transported per cell. Classical monotone flow approximations can still be used. DG methods have excellent stability properties, they can be easily constructed for arbitrary orders, and they allow simple h-p strategies to improve local approximation properties. Space-time DG methods have also been developed. We refer to the two review articles by Cheng and Shu [8] and Ekaterinaris [13] for recent comparisons and numerous further reading.

For convergence studies towards the (physically correct) entropy solution, the so-called viscous equations are often used:

$$\partial_t \mathbf{u}^\varepsilon + \partial_x \mathbf{f}(\mathbf{u}^\varepsilon) = \mathbf{g}(x, \mathbf{u}^\varepsilon) + \varepsilon \partial_{xx} \mathbf{u}^\varepsilon. \tag{51}$$

These equations are themselves a starting point for further discretizations, which are derived from the treatment of parabolic differential equations. Adding further terms, e.g. second derivatives in time, motivates the widely used *relaxation methods* for hyperbolic balance equations. An overview of the procedure and convergence results can be found in [25].

An appropriate choice of discretization method will always depend on the objective for numerical simulation, such as stability, high accuracy, low computation time, low memory, certain structure for optimization, complexity of adjoint equations, etc.

9 Port-Hamiltonian Equations

9.1 Finite Dimension

9.1.1 Ordinary Port-Hamiltonian Equations

Let $\mathcal{T}$ be a real interval, let $x : \mathcal{T} \to \mathbb{R}^n$ be the state and let $u, y : \mathcal{T} \to \in \mathbb{R}^m$ be the input and output, respectively. The simplest form of a *port-Hamiltonian system* is

$$\begin{aligned} \dot{x} &= (J - R)\nabla\mathcal{H}(x) + Gu, \\ y &= G^T\nabla\mathcal{H}(x), \end{aligned} \tag{52}$$

where

- $\mathcal{H} \in \mathcal{C}^1(\mathbb{R}^n)$ is a *Hamiltonian function* (often representing energy);
- $J = -J^T \in \mathbb{R}^{n,n}$ is the *structure matrix*;
- $R = R^T \geq 0 \in \mathbb{R}^{n,n}$ is the *dissipation matrix*;
- $G \in \mathbb{R}^{n,m}$ is the *port matrix*.

Notably, the following *power balance equation* (PBE) is satisfied along any solution:

$$\frac{\mathrm{d}}{\mathrm{d}t}\mathcal{H}(x(t)) = \nabla\mathcal{H}(x)^T\dot{x} = -\nabla\mathcal{H}(x)^T R\nabla\mathcal{H}(x) + y^T u. \tag{53}$$

The *dissipation inequality* immediately follows by positive semi-definiteness of R:

$$\frac{\mathrm{d}}{\mathrm{d}t}\mathcal{H}(x(t)) \leq y^T u. \tag{54}$$

These two properties can also be written in integral form:

$$\begin{aligned} \mathcal{H}(x(t_1)) - \mathcal{H}(x(t_0)) &= \int_{t_0}^{t_1} \big(-\nabla\mathcal{H}(x(t))^T R\nabla\mathcal{H}(x(t)) + y(t)^T u(t)\big)\mathrm{d}t \\ &\leq \int_{t_0}^{t_1} y(t)^T u(t)\mathrm{d}t. \end{aligned} \tag{55}$$

9.1.2 Port-Hamiltonian Descriptor Systems

While (52) is useful to grasp the fundamental characteristics of a pH system, we present here a formulation with far more generality. Let $t \in \mathcal{T} \subseteq \mathbb{R}$ be the time, let $x : \mathcal{T} \to \mathcal{X} \subseteq \mathbb{R}^n$ be the state, and let $u, y : \mathcal{T} \to \mathbb{R}^m$ be the input and output, respectively. Consider the following system of *differential-algebraic equations*:

$$\begin{aligned} E(x,t)\dot{x} + r(x,t) &= (J(x,t) - R(x,t))e(x,t) + (G(x,t) - P(x,t))u, \\ y &= (G(x,t) + P(x,t))^T e(x,t) + (S(x,t) - N(x,t))u, \end{aligned} \tag{56}$$

together with a *Hamiltonian function* $\mathcal{H} \in \mathcal{C}^1(\mathcal{X} \times \mathcal{T})$, where

- $E : \mathcal{X} \times \mathcal{T} \to \mathbb{R}^{\ell,n}$ is the *storage flow matrix function* (possibly singular or rectangular);
- $J, R : \mathcal{X} \times \mathcal{T} \to \mathbb{R}^{\ell,\ell}$ are the *structure* and *dissipation matrix functions*, respectively;
- $G, P : \mathcal{X} \times \mathcal{T} \to \mathbb{R}^{\ell,m}$ are the *port matrix functions*;
- $S, N : \mathcal{X} \times \mathcal{T} \to \mathbb{R}^{m,m}$ are the *feed-through matrix functions*;
- $r : \mathcal{X} \times \mathcal{T} \to \mathbb{R}^{\ell}$ is the *time flow function*;
- $e : \mathcal{X} \times \mathcal{T} \to \mathbb{R}^{\ell}$ is the *effort function*.

The system (56) is called a *port-Hamiltonian differential-algebraic equation* (in short pHDAE) or a *port-Hamiltonian descriptor system* if the following properties are satisfied:

i) The *total structure* and *total dissipation matrix functions* $L, W : \mathcal{X} \times \mathcal{T} \to \mathbb{R}^{\ell+m,\ell+m}$, defined as
$$L \coloneqq \begin{bmatrix} J & G \\ -G^T & N \end{bmatrix}, \qquad W \coloneqq \begin{bmatrix} R & P \\ -P^T & S \end{bmatrix},$$
satisfy $L = -L^T$ and $W = W^T \geq 0$ pointwise. In particular, $J = -J^T$, $N = -N^T$, $R = R^T \geq 0$ and $S = S^T \geq 0$.

ii) The flow and effort functions are related to the Hamiltonian by the following:
$$\begin{aligned} \nabla_x \mathcal{H}(x,t) &= E(x,t)^T e(x,t), \\ \frac{\partial \mathcal{H}}{\partial t}(x,t) &= r(x,t)^T e(x,t), \end{aligned}$$
for all $(x,t) \in \mathcal{X} \times \mathcal{T}$.

If these conditions are satisfied, then again a PBE and a dissipation inequality hold:
$$\frac{\mathrm{d}}{\mathrm{d}t}\mathcal{H}(x(t),t) = \nabla_x \mathcal{H}^T \dot{x} + \frac{\partial \mathcal{H}}{\partial t} = -\begin{bmatrix} e \\ u \end{bmatrix}^T W \begin{bmatrix} e \\ u \end{bmatrix} + y^T u, \tag{57}$$
$$\frac{\mathrm{d}}{\mathrm{d}t}\mathcal{H}(x(t),t) \leq y^T u. \tag{58}$$

It can be shown that any pHDAE can be made autonomous without breaking the structure. In particular, it can be helpful to write the general autonomous formulation:
$$\begin{aligned} E(x)\dot{x} &= (J(x) - R(x))e(x) + (G(x) - P(x))u, \\ y &= (G(x) + P(x))^T e(x) + (S(x) - N(x))u, \end{aligned} \tag{59}$$

with condition (ii) replaced by

ii-a) The flow and effort functions are related to the Hamiltonian by the following: $\nabla \mathcal{H}(x) = E(x)^T e(x)$, for all $x \in \mathcal{X}$.

More details can be found in [27].

9.2 Infinite Dimension

We provide a general formulation for port-Hamiltonian partial-differential equations. The definitions in this subsection may be imprecise, and have the goal of giving a quick overview of how things work in infinite dimension. In particular, while the presented formulations can be applied both to functions with regular and weak derivatives, we will never consider specific function spaces explicitly. More precise details will be included in [29].

Let $\mathcal{I}, \mathcal{T} \subseteq \mathbb{R}$ be open intervals of the real line representing space and time, respectively; furthermore, assume that $\mathcal{I} = (a, b)$ is bounded. Instead of mapping into finite-dimensional spaces $\mathbb{R}^\ell, \mathbb{R}^n, \mathbb{R}^m$, we will consider here function spaces. More precisely, the state space $\mathcal{Z}$ is a linear subspace of a vector space product $\mathcal{Z}_d \times \mathcal{Z}_b$, where $\mathcal{Z}_d$ is a vector space of functions from $\mathcal{I}$ to $\mathbb{R}^{n_d}$, and $\mathcal{Z}_b \cong \mathbb{R}^{n_b}$, for some $n_d, n_b \in \mathbb{N}_0$. In other words, $z \in \mathcal{Z}$ is of the form $z = (z_d; z_b)$, with $z_d : \mathcal{I} \to \mathbb{R}^{n_d}$ and $z_b \in \mathbb{R}^{n_b}$; the variable z_d represents quantities that are defined for any point of $\mathcal{I}$, i.e., **d**ensities, while z_b represents a finite number of quantities, for example the values at the **b**oundary. Similarly, we have a *flow space* $\mathcal{F} \subseteq \mathcal{F}_d \times \mathcal{F}_b$ and an *effort space* $\mathcal{E} \subseteq \mathcal{E}_d \times \mathcal{E}_b$ with dimensions ℓ_d, ℓ_b, and an *input space* $\mathcal{U} \subseteq \mathcal{U}_d \times \mathcal{U}_b$ and an *output space* $\mathcal{Y} \subseteq \mathcal{Y}_d \times \mathcal{Y}_b$ with dimensions m_d, m_b. Furthermore, we introduce the duality pairing/inner product

$$e^T f = \int_a^b e_d(x)^T f_d(x) \, \mathrm{d}x + e_b^T f_b,$$
$$y^T u = \int_a^b y_d(x)^T u_d(x) \, \mathrm{d}x + y_b^T u_b,$$

for all $e = (e_d, e_b) \in \mathcal{E}$, $f = (f_d, f_b) \in \mathcal{F}$, $y = (y_d, y_b) \in \mathcal{Y}$ and $u = (u_d, u_b) \in \mathcal{U}$.

In this context, if $J : \mathcal{E} \to \mathcal{F}$ is a linear operator, we say that J is *skew-symmetric* ($J = -J^T$) if $e^T J e = 0$ for all $e \in \mathcal{E}$. Similarly, we say that $R : \mathcal{E} \to \mathcal{F}$ is *symmetric* ($R = R^T$) if $e'^T R e = e^T R e'$ for all $e, e' \in \mathcal{E}$; additionally, R is *positive semidefinite* ($R \geq 0$) if $e^T R e \geq 0$ for all $e \in \mathcal{E}$, and *positive definite* ($R > 0$) if $e^T R e > 0$ for all $e \neq 0$.

Furthermore, if $G : \mathcal{U} \to \mathcal{F}$ is a linear operator, we denote by $G^T : \mathcal{E} \to \mathcal{Y}$ a linear operator satisfying $(G^T e)^T u = e^T G u$, for all $e \in \mathcal{E}$ and $u \in \mathcal{U}$. In most cases, this operator can be written in a way that resembles the transpose matrix in the finite-dimensional case, therefore the notation.

In what follows, we will denote by $\mathcal{L}(V, W)$ the vector space of linear operators from V to W, for any vector spaces V and W. In addition, we will denote by $T\mathcal{Z} \cong T\mathcal{Z}_d \times T\mathcal{Z}_b$ the *tangent bundle* of $\mathcal{Z}$; without giving formal definitions, we consider this as the "space of directions in which z can move in time", i.e., a vector space that contains the time derivative of any smooth trajectory $z : \mathcal{T} \to \mathcal{Z}$.

9.2.1 Port-Hamiltonian PDAEs

We consider here just the autonomous case, and we also assume that the port operator P and the feed-through operators S, N all vanish. This will let us keep the notation simple, and will be sufficient to cover all presented gas pipe models.

Let $z : \mathcal{T} \to \mathcal{Z}$ be the state, let $u \in \mathcal{U}$ be the input and let $y \in \mathcal{Y}$ be the output. Consider the following system of differential-algebraic equations:

$$\begin{aligned} E(z)\dot{z} &= (J(z) - R(z))e(z) + G(z)u, \\ y &= G(z)^T e(z), \end{aligned} \tag{60}$$

together with a *Hamiltonian function*

$$\mathcal{H}(z) = \int_a^b H(z_d(x), z_b, x)\mathrm{d}x,$$

where

- $E : \mathcal{Z} \to \mathcal{L}(T\mathcal{Z}, \mathcal{F})$ is the *storage flow operator*;
- $J, R : \mathcal{Z} \to \mathcal{L}(\mathcal{E}, \mathcal{F})$ are the *structure* and *dissipation operators*, respectively;
- $G : \mathcal{Z} \to \mathcal{L}(\mathcal{U}, \mathcal{F})$ is the *port operator*;
- $e : \mathcal{Z} \to \mathcal{E}$ is the *effort function*;
- $H \in \mathcal{C}^1(\mathbb{R}^{n_d} \times \mathbb{R}^{n_b} \times \mathcal{I}, \mathbb{R})$ is the *Hamiltonian density function*.

The system (60) is *port-Hamiltonian* if the following properties are satisfied:

i) $J = -J^T$ and $R = R^T \geq 0$, pointwise;

ii) The flow and effort functions are related to the Hamiltonian by

$$\frac{\delta \mathcal{H}}{\delta z}(z) = E(z)^T e(z), \qquad \forall z \in \mathcal{Z}, \tag{61}$$

where $\frac{\delta}{\delta z}$ is the *Fréchet derivative*. In other words, we have

$$\int_a^b \nabla_z H(z_d(x), z_b, x)^T \begin{bmatrix} w_d(x) \\ w_b \end{bmatrix} \mathrm{d}x = e(z)^T E(z) w,$$

for all $z \in \mathcal{Z}$ and $w \in T_z\mathcal{Z}$.

If these conditions are satisfied, a PBE and a dissipation inequality again hold:

$$\frac{\mathrm{d}}{\mathrm{d}t}\mathcal{H}(z(t)) = -e(z)^T R(z) e(z) + y^T u, \tag{62}$$

$$\frac{\mathrm{d}}{\mathrm{d}t}\mathcal{H}(z(t)) \leq y^T u. \tag{63}$$

This formulation works well to represent models with vanishing boundary conditions.

9.2.2 Condensed Port-Hamiltonian PDAEs

When boundary conditions are not vanishing, we will often have

$$e^T Je = (Ye)^T Ue, \qquad \forall e \in \mathcal{E},$$

for some linear operators $U, Y : \mathcal{E} \to \mathbb{R}^2$. When this happens, we will say that J is a *B-skew-symmetric operator* with *boundary input and output operators* U and Y, respectively. Usually Ue and Ye will depend on the values of e_d at the boundary of the domain; in that sense, they represent exchange of energy through the boundary.

For a simple example, consider the linear operator

$$J = \begin{bmatrix} 0 & D_x \\ D_x & 0 \end{bmatrix} : \begin{bmatrix} e_1 \\ e_2 \end{bmatrix} \mapsto \begin{bmatrix} \partial_x e_2 \\ \partial_x e_1 \end{bmatrix}.$$

Then we have

$$e^T Je = \begin{bmatrix} e_1 \\ e_2 \end{bmatrix}^T \begin{bmatrix} \partial_x e_2 \\ \partial_x e_1 \end{bmatrix} = \int_a^b (e_1 \partial_x e_2 + e_2 \partial_x e_1) \mathrm{d}x =$$
$$= \int_a^b \partial_x (e_1 e_2) \mathrm{d}x = (e_1 e_2)(b) - (e_1 e_2)(a),$$

for all $e : \mathcal{I} \to \mathbb{R}^2$ smooth enough[1]. We can then define $Ue := (-e_1(a), e_1(b))$ and $Ye := (e_2(a), e_2(b))$ to have $e^T JE = (Ye)^T Ue$. Note that the choice of operators U and Y is not unique.

Consider again the system (60), but this time replace condition (i) with

i-a) J is B-skew-symmetric and $R = R^T \geq 0$, pointwise.

We call the obtained system *condensed port-Hamiltonian*, or *B-port-Hamiltonian*. It can be shown that the following PBE and dissipation inequality hold:

$$\frac{\mathrm{d}}{\mathrm{d}t} \mathcal{H}(z(t)) = -e(z)^T R(z) e(z) + y_b(z)^T u_b(z) + y^T u, \tag{64}$$
$$\frac{\mathrm{d}}{\mathrm{d}t} \mathcal{H}(z(t)) \leq y_b(z)^T u_b(z) + y^T u, \tag{65}$$

where $u_b(z) = U(z)e(z)$ and $y_b(z) = Y(z)e(z)$, with $U(z)$ and $Y(z)$ boundary input and output operators associated with J, respectively.

A condensed port-Hamiltonian system can almost always[2] be completed to a port-Hamiltonian descriptor system:

$$\begin{bmatrix} E(z) \\ 0 \end{bmatrix} \dot{z} = \begin{bmatrix} J(z) & 0 \\ -U(z) & 0 \end{bmatrix} \begin{bmatrix} e(z) \\ Ye(z) \end{bmatrix} + \begin{bmatrix} G(z) & 0 \\ 0 & I \end{bmatrix} \begin{bmatrix} u \\ u_b \end{bmatrix},$$
$$\begin{bmatrix} y \\ y_b \end{bmatrix} = \begin{bmatrix} G(z)^T & 0 \\ 0 & I \end{bmatrix} \begin{bmatrix} e(z) \\ Ye(z) \end{bmatrix}. \tag{66}$$

[1] This works for $\mathcal{E} = \mathcal{C}^1(\mathcal{I})$ and $\mathcal{F} = \mathcal{C}(\mathcal{I})$, but also for Sobolev spaces.
[2] This will be discussed in greater detail in [29].

The additional algebraic equation $U(z)e(z) = u_b$ usually prescribes some boundary conditions.

10 Flow Models for Networks of Gas Pipes

10.1 The Euler equations (TA1)

The 1-D Euler equations are a system of nonlinear hyperbolic PDEs, that describe the behavior of compressible, non-viscous fluids:

$$\begin{aligned} &\partial_t \rho + \partial_x(\rho v) = 0, \\ &\partial_t(\rho v) + \partial_x(p + \rho v^2) = -\frac{\lambda}{2D}\rho v\,|v| - g\rho\partial_x h, \\ &\partial_t E + \partial_x\big((E+p)v\big) = -\frac{k_w}{D}(T - T_w), \end{aligned} \tag{TA1}$$

together with an equation of state for real gases $f(p, \rho, T) = 0$, for $x \in \mathcal{I} = [0, L]$ and $t \in \mathcal{T}$, where $L < \infty$ is the length of the pipe and $\mathcal{T} \subseteq \mathbb{R}$ is the time interval. Here ρ is the density, v the velocity of the gas, T the temperature and p the pressure. Sometimes we will denote by m the momentum, which is related to density and velocity by the formula $m = \rho v$. Furthermore, g is the gravitational constant, $h = h(x)$ is the height of the pipe, λ is the pipe friction coefficient, D is the pipe diameter, k_w is the thermal conductivity coefficient and $T_w = T_w(x)$ is the superficial temperature of the pipe. The variable $E = \rho(\frac{1}{2}v^2 + gh + c_v T)$ is the total energy density, where c_v is the specific heat. Depending on the model chosen for the equation of state, one could solve p as a function of ρ, T and substitute it in the equations. The first, second and third differential equations represent conservation of mass, momentum and energy, respectively.

We can rewrite the equations with respect to the state variables $\mathbf{z} = (\rho, v, T)$:

$$\rho_t + \partial_x(\rho v) = 0, \tag{67a}$$

$$\rho v_t + \rho\partial_x\left(\frac{1}{2}v^2 + gh\right) + p_x + \frac{\lambda}{2D}\rho v\,|v| = 0, \tag{67b}$$

$$c_v\rho T_t + c_v\rho v T_x + p v_x - \frac{\lambda}{2D}\rho v^2\,|v| + \frac{k_w}{D}(T - T_w) = 0. \tag{67c}$$

and express this also as

$$\mathbf{E}(\mathbf{z})\dot{\mathbf{z}} = \mathbf{J}(\mathbf{z})\mathbf{e}(\mathbf{z}) + \mathbf{G}\Delta T, \tag{68}$$

where $\Delta T \coloneqq T_w - T$,

$$\mathbf{E}(\mathbf{z}) = \begin{bmatrix} 1 & 0 & 0 \\ 0 & \rho & 0 \\ 0 & 0 & c_v\rho \end{bmatrix}, \qquad \mathbf{e}(\mathbf{z}) = \begin{bmatrix} \frac{1}{2}v^2 + gh + c_vT \\ v \\ 1 \end{bmatrix}, \qquad \mathbf{G} = \begin{bmatrix} 0 \\ 0 \\ \frac{k_w}{D} \end{bmatrix},$$
$$\mathbf{J}(\mathbf{z}) = \begin{bmatrix} 0 & -D_x\rho & 0 \\ -\rho D_x & 0 & -D_xp - \frac{\lambda}{2D}\rho v\,|v| + c_v\rho T_x \\ 0 & -pD_x + \frac{\lambda}{2D}\rho v\,|v| - c_v\rho T_x & 0 \end{bmatrix}.$$

Here and in what follows, we use this notation: if a (component of an) operator is written as $T = g_1 D_x g_2$, for some functions g_1, g_2, we interpret T as the operator

$$Tf = g_1 D_x g_2 f \coloneqq g_1 \partial_x (g_2 f).$$

In other words, when D_x is present in the notation together with some other function, it is to be interpreted that the other functions represent multiplication by that function, and the operators have to be applied in composition order. In particular, $\mathbf{J}(\mathbf{z})$ has the structure of a B-skew-symmetric operator, satisfying

$$\begin{aligned} \mathbf{e}^T\mathbf{J}(\mathbf{z})\mathbf{e} &= (\rho e_1 e_2 + p(\mathbf{z})e_2e_3)(0) - (\rho e_1e_2 + p(\mathbf{z})e_2e_3)(L) = \\ &= \Big(\rho e_2\Big(e_1 + \tfrac{p(\mathbf{z})}{\rho}e_3\Big)\Big)(0) - \Big(\rho e_2\Big(e_1 + \tfrac{p(\mathbf{z})}{\rho}e_3\Big)\Big)(L). \end{aligned}$$

for all $\mathbf{z}, \mathbf{e} : \mathcal{I} \times \mathcal{T} \to \mathbb{R}^3$ smooth enough. Let us consider as Hamiltonian function

$$\mathcal{H}(\mathbf{z}) = \int_0^L E(\mathbf{z}(x))\mathrm{d}x = \int_0^L \rho\Big(\frac{1}{2}v^2 + gh + c_vT\Big)\mathrm{d}x, \tag{69}$$

It is easy to check that $\nabla\mathcal{H}(\mathbf{z}) = \mathbf{E}(\mathbf{z})^T\mathbf{e}(\mathbf{z})$, therefore (68) expresses the condensed port-Hamiltonian system

$$\begin{aligned} \mathbf{E}(\mathbf{z})\dot{\mathbf{z}} &= \mathbf{J}(\mathbf{z})\mathbf{e}(\mathbf{z}) + \mathbf{G}u_p, \\ y_p &= \mathbf{G}^T\mathbf{e}(\mathbf{z}), \end{aligned} \tag{70}$$

that can be completed to the port-Hamiltonian descriptor system

$$\begin{aligned} \tilde{\mathbf{E}}(\mathbf{z})\dot{\mathbf{z}} &= \tilde{\mathbf{J}}(\mathbf{z})\tilde{\mathbf{e}}(\mathbf{z}) + \tilde{\mathbf{G}}\mathbf{u}, \\ \mathbf{y} &= \tilde{\mathbf{G}}^T\tilde{\mathbf{e}}(\mathbf{z}), \end{aligned} \tag{71}$$

where

$$\tilde{\mathbf{E}} = \begin{bmatrix} \mathbf{E} \\ 0 \end{bmatrix}, \qquad \tilde{\mathbf{J}} = \begin{bmatrix} \mathbf{J} & 0 \\ -U & 0 \end{bmatrix}, \qquad \tilde{\mathbf{e}} = \begin{bmatrix} \mathbf{e} \\ Y\mathbf{e} \end{bmatrix},$$
$$\tilde{\mathbf{G}} = \begin{bmatrix} \mathbf{G} & 0 \\ 0 & I \end{bmatrix}, \qquad \mathbf{u} = \begin{bmatrix} \Delta T \\ u_b \end{bmatrix}, \qquad \mathbf{y} = \begin{bmatrix} y_p \\ y_b \end{bmatrix}.$$

A preferred choice of boundary input and output operators is

$$U(\mathbf{z})\mathbf{e} = \begin{bmatrix} (\rho e_2)(0) \\ -(\rho e_2)(L) \end{bmatrix}, \qquad Y(\mathbf{z})\mathbf{e} = \begin{bmatrix} \left(e_1 + \frac{p(\mathbf{z})}{\rho} e_3\right)(0) \\ \left(e_1 + \frac{p(\mathbf{z})}{\rho} e_3\right)(L) \end{bmatrix},$$

that for $\mathbf{e} = \mathbf{e}(\mathbf{z})$ become

$$U(\mathbf{z})\mathbf{e}(\mathbf{z}) = \begin{bmatrix} m(0) \\ -m(L) \end{bmatrix}, \qquad Y(\mathbf{z})\mathbf{e}(\mathbf{z}) = \begin{bmatrix} \left(\frac{E+p}{\rho}\right)(0) \\ \left(\frac{E+p}{\rho}\right)(L) \end{bmatrix}.$$

This choice will be helpful for interconnecting multiple gas pipes into a network by using conservation of momentum. Indeed, in this way we can use the algebraic equation $U(\mathbf{z})\mathbf{e}(\mathbf{z}) = u_b$ to set boundary conditions for the momentum. The power balance equation is then

$$\frac{\mathrm{d}}{\mathrm{d}t}\mathcal{H}(\mathbf{z}(t)) = \frac{k_w}{D}\int_0^1 \Delta T \,\mathrm{d}x + [v(E+p)]_L^0. \tag{72}$$

10.2 Isothermal Model Hierarchy

10.2.1 Isothermal Euler Equations (ISO1)

In the isothermal case we take $T(t,x) \equiv T_0$ and we remove the third equation from the Euler equations. As a consequence, we get the following system:

$$\begin{aligned} &\partial_t \rho + \partial_x(\rho v) = 0, \\ &\partial_t(\rho v) + \partial_x(p + \rho v^2) = -\frac{\lambda}{2D}\rho v|v| - g\rho\partial_x h. \end{aligned} \tag{ISO1}$$

Since we are assuming the temperature to be constant, it sounds reasonable to take as state $\mathbf{z} = (\rho, v)$, as total energy density $E_{\mathrm{ISO}} = \rho(\frac{1}{2}v^2 + gh)$, and as Hamiltonian $\mathcal{H}_{\mathrm{ISO}} = \int_0^L E_{\mathrm{ISO}}\mathrm{d}x$. In particular, we have the (Fréchet) derivative

$$\frac{\delta\mathcal{H}_{\mathrm{ISO}}}{\delta\mathbf{z}} = \begin{bmatrix} \frac{1}{2}v^2 + gh \\ \rho v \end{bmatrix} = \begin{bmatrix} 1 & 0 \\ 0 & \rho \end{bmatrix}\begin{bmatrix} \frac{1}{2}v^2 + gh \\ v \end{bmatrix} =: \mathbf{E}(\mathbf{z})^T\mathbf{e}(\mathbf{z}). \tag{73}$$

As previously, it is easy to fit most of the terms in the port-Hamiltonian structure:

$$\mathbf{E}(\mathbf{z})\dot{\mathbf{z}} + \begin{bmatrix} 0 & D_x\rho \\ \rho D_x & \frac{\lambda}{2D}\rho|v| \end{bmatrix}\mathbf{e}(z) + \begin{bmatrix} 0 \\ \partial_x p \end{bmatrix} = 0. \tag{74}$$

Unfortunately, the $\partial_x p$ term does not fit in the $(\mathbf{J}(\mathbf{z}) - \mathbf{R}(\mathbf{z}))\mathbf{e}(\mathbf{z})$ part, so either we interpret this term as an additional input, or we need to incorporate it in some different way.

Suppose that the equation of state determines that the pressure can be written as a function of the mass (and the constant temperature), i.e., $p = p(\rho)$. If we add to E_{ISO} a

potential term $F(\rho)$ satisfying the second order ordinary differential equation $\rho F''(\rho) = p'(\rho)$, one can show that

$$\begin{aligned} E_{\mathrm{ISO1}}(\mathbf{z}) &= E_{\mathrm{ISO}}(\mathbf{z}) + F(\rho), \\ \mathcal{H}_{\mathrm{ISO1}}(\mathbf{z}) &= \int_0^L E_{\mathrm{ISO1}} \mathrm{d}x = \mathcal{H}_{\mathrm{ISO}}(\mathbf{z}) + \int_0^L F(\rho) \mathrm{d}x, \\ \frac{\delta \mathcal{H}_{\mathrm{ISO1}}}{\delta \mathbf{z}} &= \frac{\delta \mathcal{H}_{\mathrm{ISO}}}{\delta \mathbf{z}} + \begin{bmatrix} F'(\rho) \\ 0 \end{bmatrix} = \mathbf{E}(\mathbf{z})^T \mathbf{e}_{\mathrm{ISO1}}(\mathbf{z}). \end{aligned}$$

In particular, we can write the system as

$$\mathbf{E}_{\mathrm{ISO1}}(\mathbf{z})\dot{\mathbf{z}} = (\mathbf{J}_{\mathrm{ISO1}}(\mathbf{z}) - \mathbf{R}_{\mathrm{ISO1}}(\mathbf{z}))\mathbf{e}_{\mathrm{ISO1}}(\mathbf{z}), \tag{75}$$

where

$$\begin{aligned} \mathbf{E}_{\mathrm{ISO1}}(\mathbf{z}) &= \begin{bmatrix} 1 & 0 \\ 0 & \rho \end{bmatrix}, \qquad \mathbf{J}_{\mathrm{ISO1}}(\mathbf{z}) = \begin{bmatrix} 0 & -D_x\rho \\ -\rho D_x & 0 \end{bmatrix}, \\ \mathbf{R}_{\mathrm{ISO1}}(\mathbf{z}) &= \begin{bmatrix} 0 & 0 \\ 0 & \frac{\lambda}{2D}\rho|v| \end{bmatrix}, \qquad \mathbf{e}_{\mathrm{ISO1}}(\mathbf{z}) = \begin{bmatrix} \frac{1}{2}v^2 + gh + F'(\rho) \\ v \end{bmatrix}. \end{aligned}$$

From now on, we omit "ISO1" from the notation: when we write $\mathbf{e}$, we refer to the version with the $F'(\rho)$ term. Since $\mathbf{J}(\mathbf{z})$ is again a B-skew-symmetric operator satisfying

$$\mathbf{e}^T \mathbf{J}(\mathbf{z})\mathbf{e} = (\rho e_1 e_2)(0) - (\rho e_1 e_2)(L), \tag{76}$$

and clearly $\mathbf{R} = \mathbf{R}^T \geq 0$, this is a condensed port-Hamiltonian system (with no extra input and output). It can then be completed to the port-Hamiltonian descriptor system

$$\begin{aligned} \tilde{\mathbf{E}}(\mathbf{z})\dot{\mathbf{z}} &= (\tilde{\mathbf{J}}(\mathbf{z}) - \tilde{\mathbf{R}}(\mathbf{z}))\tilde{\mathbf{e}}(\mathbf{z}) + \tilde{\mathbf{G}}u_b, \\ y_b &= \tilde{\mathbf{G}}^T \tilde{\mathbf{e}}(\mathbf{z}), \end{aligned} \tag{77}$$

where

$$\tilde{\mathbf{E}} = \begin{bmatrix} \mathbf{E} \\ 0 \end{bmatrix}, \quad \tilde{\mathbf{J}} = \begin{bmatrix} \mathbf{J} & 0 \\ -U & 0 \end{bmatrix}, \quad \tilde{\mathbf{R}} = \begin{bmatrix} \mathbf{R} & 0 \\ 0 & 0 \end{bmatrix}, \quad \tilde{\mathbf{e}} = \begin{bmatrix} \mathbf{e} \\ Y\mathbf{e} \end{bmatrix}, \quad \tilde{\mathbf{G}} = \begin{bmatrix} 0 \\ I \end{bmatrix},$$

A preferred choice for boundary input and output operators is

$$U(\mathbf{z})\mathbf{e} = \begin{bmatrix} (\rho e_2)(0) \\ -(\rho e_2)(L) \end{bmatrix}, \qquad Y\mathbf{e} = \begin{bmatrix} e_1(0) \\ e_1(L) \end{bmatrix},$$

so that for $\mathbf{e} = \mathbf{e}(\mathbf{z})$ we have

$$U(\mathbf{z})\mathbf{e}(\mathbf{z}) = \begin{bmatrix} m(0) \\ -m(L) \end{bmatrix}, \qquad Y\mathbf{e}(\mathbf{z}) = \begin{bmatrix} \left(\frac{1}{2}v^2 + gh + F'(\rho)\right)(0) \\ \left(\frac{1}{2}v^2 + gh + F'(\rho)\right)(L) \end{bmatrix}.$$

The algebraic equation $U(\mathbf{z})\mathbf{e}(\mathbf{z}) = u_b$ prescribes the boundary conditions for the momentum. The power balance equation is then

$$\frac{\mathrm{d}}{\mathrm{d}t}\mathcal{H}(\mathbf{z}(t)) = -\frac{\lambda}{2D}\int_0^L \rho\,|v|\,v^2\,\mathrm{d}x + \left[\rho v\left(\frac{1}{2}v^2 + gh + F'(\rho)\right)\right]_L^0.$$

One can show that $F(\rho)$ solves its defining ODE if and only if it is of the form

$$F(\rho) = \iint \frac{p'(\rho)}{\rho}\mathrm{d}\rho + c_1\rho + c_0, \tag{78}$$

for some constants $c_1, c_0 \in \mathbb{R}$. In particular, one can deduce that $\rho F'(\rho) = F(\rho) + p(\rho)$, up to an additive constant. Therefore, for a particular choice of $c_0 \in \mathbb{R}$, the PBE is actually

$$\frac{\mathrm{d}}{\mathrm{d}t}\mathcal{H}(\mathbf{z}(t)) = -\frac{\lambda}{2D}\int_0^L \rho\,|v|\,v^2\,\mathrm{d}x + [v(E+p)]_L^0,$$

which should be preferred because of consistency with (TA1).

We present explicit choices $F(\rho)$, for two commonly used equations of state:

- Suppose that the equation of state is $p = R\rho T(1+\alpha p)$, for some constant α. Since the temperature $T \equiv T_0$ is constant, we can write p as a function of ρ:

$$p(\rho) = \frac{RT_0\rho}{1 - \alpha RT_0\rho}. \tag{79}$$

  A solution of the defining ODE for $F(\rho)$ is then $F(\rho) = RT_0\rho\log p$, that conveniently satisfies $\rho F'(\rho) = F(\rho) + p$.

- If the gas is ideal, then $p = RT\rho$, i.e., $\alpha = 0$. Instead of taking $RT_0\rho\log p$ as before, one can also equivalently take $F(\rho) = RT_0\rho\log\rho$, which satisfies both the ODE and the relation $\rho F'(\rho) = F(\rho) + p$.

10.2.2 Semilinear Model (ISO2)

Assume that the equation of state can be approximated by $p = c^2\rho$ for some constant $c > 0$; in particular, from now on we will take $F(\rho) = c^2\rho\log\rho$ and $F'(\rho) = c^2(\log\rho + 1)$. The term in the spatial derivative of the second equation of (ISO1) can then be written as

$$p + \rho v^2 = p\left(1 + \frac{v^2}{c^2}\right).$$

For small flow velocity $|v| \ll c$, one can approximate the term in brackets with 1 and get the following semilinear model:

$$\begin{aligned} &\partial_t\rho + \partial_x(\rho v) = 0, \\ &\partial_t(\rho v) + \partial_x p = -\frac{\lambda}{2D}\rho v\,|v| - g\rho\partial_x h. \end{aligned} \tag{ISO2}$$

Alternatively, this model can be reached assuming $\partial_x(\rho v^2)$ to be negligibly small; in that case, no assumption is necessary for the equation of state. If we take as previously $E(\mathbf{z}) = \frac{1}{2}\rho v^2 + \rho g h + F(\rho)$ and $\mathcal{H}(\mathbf{z}) = \int_0^L E(\mathbf{z})\mathrm{d}x$, conservation properties are unfortunately lost. This happens because the cancellation of the term $\partial_x(\rho v^2)$ breaks the port-Hamiltonian structure. In fact, the system can now be written as

$$\mathbf{E}(\mathbf{z})\dot{\mathbf{z}} = \begin{bmatrix} 0 & -D_x\rho \\ -\rho D_x & -\frac{\lambda}{2D}\rho|v| + D_x\rho v \end{bmatrix}\mathbf{e}(\mathbf{z}) \tag{80}$$

The problem is in the $D_x\rho v$ entry of the matrix, that can be shown to be indefinite.

One possible solution is to look for a different total energy density (thus a new Hamiltonian). When the effect of gravity is negligible, this can be successfully done, but the dimension and interpretation of energy is different. This will be discussed in more detail in subsection 10.4.

10.2.3 Semilinear Model (ISO2F)

The model (ISO2F) admits a port-Hamiltonian structure, not with respect to the original Hamiltonian but with respect to a quadratic Hamiltonian that can be thought of as an approximation of the original Hamiltonian. We have

$$\begin{pmatrix} \frac{\partial \rho_1}{\partial \tau} \\ \frac{\partial w}{\partial \tau} \end{pmatrix} = \left(\begin{pmatrix} 0 & -\frac{\partial}{\partial x} \\ -\frac{\partial}{\partial x} & 0 \end{pmatrix} - \begin{pmatrix} 0 & 0 \\ 0 & \frac{|w|}{2\rho_0} \end{pmatrix} \right) \begin{pmatrix} \frac{p'(\rho_0)}{\rho_0}\rho_1 \\ \rho_0 w \end{pmatrix} \tag{81}$$

and therefore

$$\frac{\partial \mathbf{z}}{\partial \tau} = (\mathcal{J} - \mathcal{R}(\mathbf{z}))\mathcal{H}'(\mathbf{z}), \quad \mathcal{H}(\mathbf{z}) = \frac{1}{2}\int_0^L \frac{p'(\rho_0)}{\rho_0}\rho_1^2 + \rho_0 w^2\, dx \tag{82}$$

with $\mathbf{z} = (\rho_1, w)^T$.

10.2.4 The Friction Dominated Model (ISO3)

One possible solution to restore the port-Hamiltonian structure of (ISO2) is to remove a second term. If we assume that $\partial_t(\rho v)$ is small enough, so that it can be neglected, we get the so-called friction dominated model:

$$\begin{aligned} &\partial_t \rho + \partial_x(\rho v) = 0, \\ &\partial_x p = -\frac{\lambda}{2D}\rho v|v| - g\rho\partial_x h. \end{aligned} \tag{ISO3}$$

This can be written equivalently as

$$\mathbf{E}_{\mathrm{ISO3}}\dot{\mathbf{z}} = (\mathbf{J}_{\mathrm{ISO1}}(\mathbf{z}) - \mathbf{R}_{\mathrm{ISO1}}(\mathbf{z}))\mathbf{e}_{\mathrm{ISO3}}(\mathbf{z}), \tag{83}$$

where $\mathbf{J}_{\mathrm{ISO1}}(\mathbf{z})$ and $\mathbf{R}_{\mathrm{ISO1}}(\mathbf{z})$ are the same as in (ISO1), and

$$\mathbf{E}_{\mathrm{ISO3}} = \begin{bmatrix} 1 & 0 \\ 0 & 0 \end{bmatrix}, \qquad \mathbf{e}_{\mathrm{ISO3}}(\mathbf{z}) = \begin{bmatrix} gh + F'(\rho) \\ v \end{bmatrix}.$$

This is a condensed port-Hamiltonian descriptor system with associated Hamiltonian function

$$\mathcal{H}_{\mathrm{ISO3}}(\mathbf{z}) = \int_0^L E_{\mathrm{ISO3}}(\mathbf{z}(x))\mathrm{d}x \coloneqq \int_0^L (\rho g h + F(\rho))\mathrm{d}x, \tag{84}$$

since

$$\frac{\delta \mathcal{H}_{\mathrm{ISO3}}}{\delta \mathbf{z}} = \begin{bmatrix} gh + F'(\rho) \\ 0 \end{bmatrix} = \mathbf{E}_{\mathrm{ISO3}}(\mathbf{z})^T \mathbf{e}_{\mathrm{ISO3}}(\mathbf{z}).$$

In other words, neglecting $\partial_x(\rho v^2)$ and $\partial_t(\rho v)$ has the natural consequence of neglecting the kinetic term of the Hamiltonian too.

Let us omit "ISO3" from the notation, for simplicity. We can complete this system to a port-Hamiltonian descriptor system in the usual way. The choice of boundary input and output operators $U(\mathbf{z}), Y$ is the same as for (ISO1). In particular, for $\mathbf{e} = \mathbf{e}(\mathbf{z})$ we have

$$U(\mathbf{z})\mathbf{e}(\mathbf{z}) = \begin{bmatrix} m(0) \\ -m(L) \end{bmatrix}, \qquad Y\mathbf{e}(\mathbf{z}) = \begin{bmatrix} (gh + F'(\rho))(0) \\ (gh + F'(\rho))(L) \end{bmatrix},$$

the algebraic equation $U(\mathbf{z})\mathbf{e}(\mathbf{z}) = u_b$ sets the boundary conditions for the momentum, and the power balance equation is again

$$\frac{\mathrm{d}}{\mathrm{d}t}\mathcal{H}(\mathbf{z}(t)) = -\frac{\lambda}{2D}\int_0^L \rho\,|v|\,v^2\,\mathrm{d}x + \left[v(E+p)\right]_L^0.$$

10.2.5 Algebraic Equations (ISO4)

In the stationary case, the other time derivative also disappears. Neglecting gravitation, we get the algebraic equations

$$\begin{aligned} &\partial_x(\rho v) = 0, \\ &\partial_x p = -\frac{\lambda}{2D}\rho v\,|v|\,. \end{aligned} \tag{ISO4}$$

Although the system has stationary dynamics, we can still interpret it as a condensed port-Hamiltonian descriptor system of the form

$$\mathbf{0} = (\mathbf{J}_{\mathrm{ISO1}}(\mathbf{z}) - \mathbf{R}_{\mathrm{ISO1}}(\mathbf{z}))\mathbf{e}_{\mathrm{ISO4}}(\mathbf{z}), \tag{85}$$

with $\mathbf{E}_{\mathrm{ISO4}} = \mathbf{0}$, $\mathbf{e}_{\mathrm{ISO4}}(\mathbf{z}) = (F'(\rho), v)$, and all other coefficients defined as in (ISO1), together with a trivial Hamiltonian $\mathcal{H}_{\mathrm{ISO4}}(\mathbf{z}) = \mathrm{const}$.

Let us omit "ISO4" from the notation, for simplicity. We can complete this system to a purely algebraic port-Hamiltonian descriptor system

$$\begin{aligned} \mathbf{0} &= (\tilde{\mathbf{J}}(\mathbf{z}) - \tilde{\mathbf{R}}(\mathbf{z}))\tilde{\mathbf{e}}(\mathbf{z}) + \tilde{\mathbf{G}}u_b, \\ y_b &= \tilde{\mathbf{G}}^T\tilde{\mathbf{e}}(\mathbf{z}). \end{aligned} \tag{86}$$

The boundary input and output operators $U(\mathbf{z}), Y$ are chosen as in (ISO3). In particular, for $\mathbf{e} = \mathbf{e}(\mathbf{z})$ we have

$$U(\mathbf{z})\mathbf{e}(\mathbf{z}) = \begin{bmatrix} m(0) \\ -m(L) \end{bmatrix}, \qquad Y\mathbf{e}(\mathbf{z}) = \begin{bmatrix} (F'(\rho))(0) \\ (F'(\rho))(L) \end{bmatrix},$$

the algebraic equation $U(\mathbf{z})\mathbf{e}(\mathbf{z}) = u_b$ sets the boundary conditions for the momentum, and the power balance equation is

$$0 = -\frac{\lambda}{2D}\int_0^L \rho\,|v|\,v^2\,\mathrm{d}x + \left[v(F(\rho)+p)\right]_L^0.$$

Although there is no dynamics involved, the port-Hamiltonian formulation of (ISO4) is still useful for energy-preserving interconnection.

10.3 Non-Isothermal Model Hierarchy

10.3.1 Simplified Nonlinear Equations (TA2)

Starting from the Euler equations, let us assume that for small velocities the time and space derivatives of ρv^2 and ρv^3 are negligibly small. This results in the model

$$\begin{aligned} &\partial_t\rho + \partial_x(\rho v) = 0, \\ &\partial_t(\rho v) + \partial_x p = -\frac{\lambda}{2D}\rho v\,|v| - g\rho\partial_x h, \\ &\partial_t E_{\mathrm{TA2}} + \partial_x\big((E_{\mathrm{TA2}} + p)v\big) = -\frac{k_w}{D}(T - T_w), \end{aligned} \tag{TA2}$$

where $E_{\mathrm{TA2}} = \rho g h + c_v\rho T$ replaces the total energy density $E_{\mathrm{TA1}} = \frac{1}{2}\rho v^2 + \rho g h + c_v\rho T$. In other words, the kinetic term has been removed from the total energy, since ρv^2 is neglibly small. With that in mind, we define as Hamiltonian function

$$\mathcal{H}_{\mathrm{TA2}} = \int_0^L E_{\mathrm{TA2}}(\mathbf{z})\mathrm{d}x = \int_0^L (\rho g h + c_v\rho T)\mathrm{d}x. \tag{87}$$

The Fréchet derivative of $\mathcal{H}_{\mathrm{TA2}}$ is then

$$\delta\mathcal{H}_{\mathrm{TA2}} = \begin{bmatrix} gh + c_v T \\ 0 \\ c_v\rho \end{bmatrix} = \begin{bmatrix} 1 & 0 & 0 \\ 0 & 1 & 0 \\ 0 & 0 & c_v\rho \end{bmatrix}\begin{bmatrix} gh + c_v T \\ 0 \\ 1 \end{bmatrix}. \tag{88}$$

(TA2) can be rewritten equivalently as

$$\begin{aligned} \partial_t \rho &= -\partial_x(\rho v), \\ \rho \partial_t v &= v\partial_x(\rho v) - \partial_x p - \frac{\lambda}{2D}\rho v\,|v| - g\rho\partial_x h, \\ c_v \rho \partial_t T &= -\rho v \partial_x(gh + c_v T) - \partial_x(pv) + \frac{k_w}{D}\Delta T, \end{aligned} \tag{89}$$

that can be written as the condensed port-Hamiltonian system

$$\begin{aligned} \mathbf{E}_{\mathrm{TA2}}(\mathbf{z})\dot{\mathbf{z}} &= \mathbf{J}_{\mathrm{TA2}}(\mathbf{z})\mathbf{e}_{\mathrm{TA2}}(\mathbf{z}) + \mathbf{G}_{\mathrm{TA2}} u_p, \\ y_p &= \mathbf{G}_{\mathrm{TA2}}^T \mathbf{e}_{\mathrm{TA2}}(\mathbf{z}), \end{aligned} \tag{90}$$

where $u_p = \Delta T$,

$$\mathbf{E}_{\mathrm{TA2}}(\mathbf{z}) = \begin{bmatrix} 1 & 0 & 0 \\ 0 & 1 & 0 \\ 0 & 0 & c_v\rho \end{bmatrix}, \quad \mathbf{e}_{\mathrm{TA2}}(\hat{\mathbf{z}}) = \begin{bmatrix} gh + c_v T \\ 0 \\ 1 \end{bmatrix}, \quad \mathbf{G}_{\mathrm{TA2}}(\hat{\mathbf{z}}) = \begin{bmatrix} 0 \\ 0 \\ \frac{k_w}{D} \end{bmatrix},$$

and

$$\mathbf{J}_{\mathrm{TA2}}(\mathbf{z}) = \begin{bmatrix} 0 & 0 & -D_x\rho v \\ 0 & 0 & J_{23}(\mathbf{z}) \\ -\rho v D_x & -J_{23}(\mathbf{z}) & J_{33}(\mathbf{z}) \end{bmatrix},$$

with

$$\begin{aligned} J_{23}(\mathbf{z}) &= v\partial_x(\rho v) - \partial_x p - \frac{\lambda}{2D}\rho v\,|v| - g\rho\partial_x h, \\ J_{33}(\mathbf{z}) &= -pvD_x - D_x pv, \end{aligned}$$

satisfies

$$\begin{aligned} \mathbf{e}^T\mathbf{J}(\mathbf{z})\mathbf{e} &= (\rho v e_1 e_3 + p v e_3 e_3)(0) - (\rho v e_1 e_3 + p v e_3 e_3)(L) = \\ &= \left(\rho v e_3\left(e_1 + \tfrac{p}{\rho}e_3\right)\right)(0) - \left(\rho v e_3\left(e_1 + \tfrac{p}{\rho}e_3\right)\right)(L). \end{aligned}$$

Let us omit "TA2" from the notation, for simplicity. We can complete this system to a port-Hamiltonian descriptor system

$$\begin{aligned} \tilde{\mathbf{E}}(\mathbf{z})\dot{\mathbf{z}} &= \tilde{\mathbf{J}}(\mathbf{z})\tilde{\mathbf{e}}(\mathbf{z}) + \tilde{\mathbf{G}}\mathbf{u}, \\ \mathbf{y} &= \tilde{\mathbf{G}}^T\tilde{\mathbf{e}}(\mathbf{z}), \end{aligned} \tag{91}$$

where

$$\tilde{\mathbf{E}} = \begin{bmatrix} \mathbf{E} \\ 0 \end{bmatrix}, \qquad \tilde{\mathbf{J}} = \begin{bmatrix} -\mathbf{J} & 0 \\ -U & 0 \end{bmatrix}, \qquad \tilde{\mathbf{e}} = \begin{bmatrix} \mathbf{e} \\ Y\mathbf{e} \end{bmatrix},$$
$$\tilde{\mathbf{G}} = \begin{bmatrix} \mathbf{G} & 0 \\ 0 & I \end{bmatrix}, \qquad \mathbf{u} = \begin{bmatrix} \Delta T \\ u_b \end{bmatrix}, \qquad \mathbf{y} = \begin{bmatrix} y_p \\ y_b \end{bmatrix}.$$

Our preferred choice of boundary input and output operators is

$$U(\mathbf{z})\mathbf{e} = \begin{bmatrix} (\rho v e_3)(0) \\ -(\rho v e_3)(L) \end{bmatrix}, \qquad Y(\mathbf{z})\mathbf{e} = \begin{bmatrix} \left(e_1 + \frac{p}{\rho} e_3\right)(0) \\ \left(e_1 + \frac{p}{\rho} e_3\right)(L) \end{bmatrix},$$

that for $\mathbf{e} = \mathbf{e}(\mathbf{z})$ becomes

$$U(\mathbf{z})\mathbf{e}(\mathbf{z}) = \begin{bmatrix} (\rho v)(0) \\ -(\rho v)(L) \end{bmatrix}, \qquad Y(\mathbf{z})\mathbf{e}(\mathbf{z}) = \begin{bmatrix} \left(\frac{E+p}{\rho}\right)(0) \\ \left(\frac{E+p}{\rho}\right)(L) \end{bmatrix},$$

The algebraic equation $U(\mathbf{z})\mathbf{e}(\mathbf{z}) = u_b$ sets the boundary conditions for the momentum, and the power balance equation is again

$$\frac{\mathrm{d}}{\mathrm{d}t}\mathcal{H}(\mathbf{z}(t)) = \frac{k_w}{D}\int_0^1 \Delta T \,\mathrm{d}x + [v(E+p)]_L^0. \tag{92}$$

10.3.2 Further Simplified Nonlinear Equations (TA3)

If one assumes that the time derivative $\partial_t(\rho v)$ is also neglibly small, then we get the model

$$\begin{aligned} &\partial_t \rho + \partial_x(\rho v) = 0, \\ &\partial_x p = -\frac{\lambda}{2D}\rho v\,|v| - g\rho\partial_x h, \\ &\partial_t E_{\mathrm{TA2}} + \partial_x\big((E_{\mathrm{TA2}} + p)v\big) = -\frac{k_w}{D}(T - T_w). \end{aligned} \tag{TA3}$$

One possible condensed port-Hamiltonian formulation results from modifying (TA1):

$$\begin{aligned} \mathbf{E}_{\mathrm{TA3}}(\mathbf{z})\dot{\mathbf{z}} &= \mathbf{J}_{\mathrm{TA1}}(\mathbf{z})\mathbf{e}_{\mathrm{TA3}}(\mathbf{z}) + \mathbf{G}_{\mathrm{TA1}}u_p, \\ y_p &= \mathbf{G}_{\mathrm{TA1}}^T\mathbf{e}_{\mathrm{TA3}}(\mathbf{z}), \end{aligned} \tag{93}$$

where $\mathbf{e}_{\mathrm{TA3}}(\mathbf{z}) = (gh + c_v T, v, 1)$ and $u_p = \Delta T$. Let us omit "TA1" and "TA3" from the notation, for simplicity. Since $\mathbf{J}(\mathbf{z})$ is the same as in (TA1), we can pick the same boundary operators U, Y. We can then complete this system to a port-Hamiltonian descriptor system

$$\begin{aligned} \tilde{\mathbf{E}}(\mathbf{z})\dot{\mathbf{z}} &= \tilde{\mathbf{J}}(\mathbf{z})\tilde{\mathbf{e}}(\mathbf{z}) + \tilde{\mathbf{G}}\mathbf{u}, \\ \mathbf{y} &= \tilde{\mathbf{G}}^T\tilde{\mathbf{e}}(\mathbf{z}), \end{aligned} \tag{94}$$

where

$$\tilde{\mathbf{E}} = \begin{bmatrix} \mathbf{E} \\ 0 \end{bmatrix}, \qquad \tilde{\mathbf{J}} = \begin{bmatrix} -\mathbf{J} & 0 \\ -U & 0 \end{bmatrix}, \qquad \tilde{\mathbf{e}} = \begin{bmatrix} \mathbf{e} \\ Y\mathbf{e} \end{bmatrix},$$
$$\tilde{\mathbf{G}} = \begin{bmatrix} \mathbf{G} & 0 \\ 0 & I \end{bmatrix}, \qquad \mathbf{u} = \begin{bmatrix} \Delta T \\ u_b \end{bmatrix}, \qquad \mathbf{y} = \begin{bmatrix} y_p \\ y_b \end{bmatrix}.$$

The algebraic equation $U(\mathbf{z})\mathbf{e}(\mathbf{z}) = u_b$ prescribes as usual the boundary conditions for the momentum, and the power balance equation is again

$$\frac{\mathrm{d}}{\mathrm{d}t}\mathcal{H}(\mathbf{z}(t)) = \frac{k_w}{D}\int_0^1 \Delta T \,\mathrm{d}x + [(E+p)v]_L^0. \tag{95}$$

10.3.3 Stationary Model (TA4)

As a further step, we can consider the stationary case, where all quantities are assumed to be constant in time, and gravity has been neglected:

$$\begin{aligned} &\partial_x(\rho v) = 0, \\ &\partial_x p = -\frac{\lambda}{2D}\rho v\,|v|\,, \\ &\partial_x\big((E_{\mathrm{TA2}}+p)v\big) = -\frac{k_w}{D}(T - T_w). \end{aligned} \tag{TA4}$$

We can assign a (purely algebraic) port-Hamiltonian formulation, by defining a constant function $\mathcal{H}_{\mathrm{TA4}} \equiv$ const. as the Hamiltonian, and modifying (TA3) by replacing $\mathbf{E}$ with the zero matrix. In particular, we can write the algebraic condensed port-Hamiltonian system

$$\begin{aligned} \mathbf{0} &= \mathbf{J}_{\mathrm{TA1}}(\mathbf{z})\mathbf{e}_{\mathrm{TA3}}(\mathbf{z}) + \mathbf{G}_{\mathrm{TA1}}u_p, \\ y_p &= \mathbf{G}_{\mathrm{TA1}}^T\mathbf{e}_{\mathrm{TA3}}(\mathbf{z}), \end{aligned} \tag{96}$$

and pick the same boundary operators U, Y as for (TA1). Let us omit "TA1" and "TA3" from the notation, for simplicity. We can complete this system to a port-Hamiltonian descriptor system

$$\begin{aligned} \mathbf{0} &= \tilde{\mathbf{J}}(\mathbf{z})\tilde{\mathbf{e}}(\mathbf{z}) + \tilde{\mathbf{G}}\mathbf{u}, \\ \mathbf{y} &= \tilde{\mathbf{G}}^T\tilde{\mathbf{e}}(\mathbf{z}), \end{aligned} \tag{97}$$

where

$$\tilde{\mathbf{E}} = \begin{bmatrix}\mathbf{E} \\ 0\end{bmatrix}, \qquad \tilde{\mathbf{J}} = \begin{bmatrix}-\mathbf{J} & 0 \\ -U & 0\end{bmatrix}, \qquad \tilde{\mathbf{e}} = \begin{bmatrix}\mathbf{e} \\ Y\mathbf{e}\end{bmatrix},$$
$$\tilde{\mathbf{G}} = \begin{bmatrix}\mathbf{G} & 0 \\ 0 & I\end{bmatrix}, \qquad \mathbf{u} = \begin{bmatrix}\Delta T \\ u_b\end{bmatrix}, \qquad \mathbf{y} = \begin{bmatrix}y_p \\ y_b\end{bmatrix}.$$

The algebraic equation $U(\mathbf{z})\mathbf{e}(\mathbf{z}) = u_b$ prescribes as usual the boundary conditions for the momentum, and the power balance equation is again

$$\frac{\mathrm{d}}{\mathrm{d}t}\mathcal{H}(\mathbf{z}(t)) = \frac{k_w}{D}\int_0^1 \Delta T \,\mathrm{d}x + [(E_{\mathrm{TA2}}+p)v]_0^L. \tag{98}$$

10.3.4 Temperature-Dependent Algebraic Model (TA4b)

In the old model hierarchy, an additional step is provided by taking as equation of state $p = c^2\rho$. Although this is allows for an explicit solution of the resulting PDAE, nothing changes from a pH perspective.

10.4 Alternative Port-Hamiltonian Formulations

When neglecting the gravitational term, it can be shown that the models (ISO2), (ISO3) and (ISO4) admit an alternative port-Hamiltonian formulation.

10.4.1 Alternative Semilinear Model (ISO2b)

Let us consider again the equations defining (ISO2), but this time neglecting the gravitational term:

$$\begin{aligned} &\partial_t \rho + \partial_x m = 0, \\ &\partial_t m + \partial_x p = -\frac{\lambda}{2D}\,|v|\,m. \end{aligned} \tag{ISO2b}$$

This system can be equivalently written as

$$\dot{\hat{\mathbf{z}}} = (\mathbf{J}_{\mathrm{ISO2b}} - \mathbf{R}_{\mathrm{ISO2b}}(\hat{\mathbf{z}}))\mathbf{e}_{\mathrm{ISO2b}}(\hat{\mathbf{z}}), \tag{99}$$

where $\hat{\mathbf{z}} = (\rho, m)$ and

$$\mathbf{J}_{\mathrm{ISO2b}} = \begin{bmatrix} 0 & -D_x \\ -D_x & 0 \end{bmatrix}, \quad \mathbf{R}_{\mathrm{ISO2b}}(\hat{\mathbf{z}}) = \begin{bmatrix} 0 & 0 \\ 0 & \frac{\lambda}{2D}|v| \end{bmatrix}, \quad \mathbf{e}_{\mathrm{ISO2b}}(\hat{\mathbf{z}}) = \begin{bmatrix} p \\ m \end{bmatrix}.$$

The operator $\mathbf{J}_{\mathrm{ISO2b}}(\hat{\mathbf{z}})$ is B-skew-symmetric with

$$\mathbf{e}^T \mathbf{J}_{\mathrm{ISO2b}}(\hat{\mathbf{z}})\mathbf{e} = (e_1 e_2)(0) - (e_1 e_2)(L), \tag{100}$$

while $\mathbf{R}_{\mathrm{ISO2b}} = \mathbf{R}_{\mathrm{ISO2b}}^T \geq 0$. Furthermore, since $p(\rho) = c^2\rho$, if we take as Hamiltonian

$$\mathcal{H}_{\mathrm{ISO2b}}(\hat{\mathbf{z}}) = \int_0^L \left(\frac{c^2}{2}\rho^2 + \frac{1}{2}m^2\right)\mathrm{d}x, \tag{101}$$

we deduce $\frac{\delta \mathcal{H}_{\mathrm{ISO2b}}}{\delta \hat{\mathbf{z}}} = \mathbf{e}_{\mathrm{ISO2b}}(\hat{\mathbf{z}})$. Therefore, (99) is a condensed port-Hamiltonian system.

From now on, let us omit "ISO2b" from the notation. Consistently with our previous choices, we take as boundary input and output operators

$$U\mathbf{e} = \begin{bmatrix} e_2(0) \\ -e_2(L) \end{bmatrix}, \qquad Y\mathbf{e} = \begin{bmatrix} e_1(0) \\ e_1(L) \end{bmatrix},$$

so that, for $\mathbf{e} = \mathbf{e}(\hat{\mathbf{z}})$,

$$U\mathbf{e}(\hat{\mathbf{z}}) = \begin{bmatrix} m(0) \\ -m(L) \end{bmatrix}, \qquad Y\mathbf{e}(\hat{\mathbf{z}}) = \begin{bmatrix} p(0) \\ p(L) \end{bmatrix}.$$

If we complete the system to a port-Hamiltonian in the usual way, the additional algebraic equation $U\mathbf{e}(\hat{\mathbf{z}}) = u_b$ prescribes the boundary momentum, and the power balance equation is

$$\frac{\mathrm{d}}{\mathrm{d}t}\mathcal{H}_{\mathrm{ISO2b}}(\hat{\mathbf{z}}(t)) = -\frac{\lambda}{2D}\int_0^L |v|\, m^2 \mathrm{d}x + [mp]_L^0. \tag{102}$$

10.4.2 Alternative Friction Dominated Model (ISO3b)

Let us consider again the equations defining (ISO3), but this time neglecting the gravitational term:

$$\begin{aligned} &\partial_t \rho + \partial_x m = 0, \\ &\partial_x p = -\frac{\lambda}{2D}|v|\, m. \end{aligned} \tag{ISO3b}$$

Instead of deriving the pH formulation inherited from (ISO1), we notice that this can be written equivalently as

$$\mathbf{E}_{\mathrm{ISO3b}}\dot{\hat{\mathbf{z}}} = (\mathbf{J}_{\mathrm{ISO2b}} - \mathbf{R}_{\mathrm{ISO2b}}(\hat{\mathbf{z}}))\mathbf{e}_{\mathrm{ISO2b}}(\hat{\mathbf{z}}), \tag{103}$$

where $\mathbf{E}_{\mathrm{ISO3b}} = \left[\begin{smallmatrix} 1 & 0 \\ 0 & 0 \end{smallmatrix}\right]$ and the other coefficients are the same as in (ISO2b). If we take as Hamiltonian

$$\mathcal{H}_{\mathrm{ISO3b}}(\hat{\mathbf{z}}) = \int_0^L \frac{c^2}{2}\rho^2 \,\mathrm{d}x, \tag{104}$$

then its Fréchet derivative satisfies $\frac{\delta \mathcal{H}}{\delta \hat{\mathbf{z}}} = (p, m) = \mathbf{E}_{\mathrm{ISO3b}}^T \mathbf{e}_{\mathrm{ISO2b}}(\hat{\mathbf{z}})$. Therefore, (103) is again a condensed port-Hamiltonian system. The choice of the boundary input and output operators U, Y can be made in the same way as in (ISO2b). Thus, the additional algebraic equation that we get when making the system a port-Hamiltonian descriptor prescribes as usual boundary conditions for the momentum, and we get the same power balance equation.

10.4.3 Alternative Algebraic Equations (ISO4b)

Let us consider again the equations defining (ISO4):

$$\begin{aligned} &\partial_x m = 0, \\ &\partial_x p = -\frac{\lambda}{2D}|v|\, m. \end{aligned} \tag{ISO4b}$$

Without even changing the Hamiltonian $\mathcal{H}_{\text{ISO4}} \equiv \text{const.}$, we notice that this system can also be written as

$$0 = (\mathbf{J}_{\text{ISO2b}} - \mathbf{R}_{\text{ISO2b}}(\hat{\mathbf{z}}))\mathbf{e}_{\text{ISO2b}}(\hat{\mathbf{z}}), \tag{105}$$

which is a purely algebraic condensed port-Hamiltonian system with $\mathbf{E}_{\text{ISO4b}} = 0$. The same choice of boundary input and output operators U, Y as in (ISO2b) leads to prescribing boundary conditions for the momentum and to the power balance equation

$$0 = -\frac{\lambda}{2D}\int_0^L |v|\, m^2 \mathrm{d}x + [mp]_L^0. \tag{106}$$

10.4.4 Considerations on the Alternative Formulations

While the presented alternative systems can be useful on their own, one must be careful when mixing them with the previously introduced standard pH formulations. In fact, while the Hamiltonians of (TA1), (ISO1), (ISO3), (ISO4), (TA2), (TA3) and (TA4) are all clearly related and have the same dimension, and the same can be said for (ISO2b), (ISO3b) and (ISO4b) when considered as their own isolated family, if we compare for example (ISO1) and (ISO2b), we realize that their Hamiltonians represent different kind of energies, since the kinetic energy term in the former model is $\frac{1}{2}\rho v^2$, and in the latter is $\frac{1}{2}\rho^2 v^2$.

More precisely, one can observe that the alternative pH formulations are closely related to the acoustic wave equations, that can be obtained from the equation of state, conservation of mass and conservation of momentum, via linearization. Such linearization is based on the assumption that condensation (change in density for a given ambient fluid density) is very small. In other words, that the gas density keeps very close to a constant value ρ_0. To bring the alternative Hamiltonian closer to the physical energy, one possible solution would be to estimate ρ_0 and use e.g. $\frac{1}{\rho_0}\mathcal{H}_{\text{ISO2b}}$ instead of $\mathcal{H}_{\text{ISO2b}}$, so that the kinetic term $\frac{1}{2\rho_0}\rho^2 v^2 \approx \frac{1}{2}\rho v^2$ approximates the kinetic energy.

11 Energy-Preserving Interconnection

This section is just a draft, it will be expanded in the future.

Consider a network of gas pipes represented by a graph $G = (\mathcal{V}, \mathcal{E})$, where the vertices $\mathcal{V} = \{v_1, \dots, v_V\}$ are junctions, and the edges $\mathcal{E} = \{e_1, \dots, e_E\}$ are pipes. Assume for simplicity that there is no exchange of temperature with the pipe surface ($\Delta T \equiv 0$), and let us model every gas pipe as a port-Hamiltonian descriptor system:

$$\begin{aligned} \mathbf{E}_j(\mathbf{z}_j)\dot{\mathbf{z}}_j &= (\mathbf{J}_j(\mathbf{z}_j) - \mathbf{R}_j(\mathbf{z}_j))\mathbf{e}_j(\mathbf{z}_j) + \mathbf{G}_j\mathbf{u}_j, \\ \mathbf{y}_j &= \mathbf{G}_j^T\mathbf{e}_j(\mathbf{z}_j), \end{aligned} \tag{107}$$

together with a Hamiltonian function $\mathcal{H}_j(\mathbf{z}_j)$, for $j = 1, \dots, E$. We can consider now the aggregated system

$$\begin{aligned} \mathbf{E}(\mathbf{z})\dot{\mathbf{z}} &= (\mathbf{J}(\mathbf{z}) - \mathbf{R}(\mathbf{z}))\mathbf{e}(\mathbf{z}) + \mathbf{G}\mathbf{u}, \\ \mathbf{y} &= \mathbf{G}^T\mathbf{e}(\mathbf{z}), \end{aligned} \tag{108}$$

obtained by stacking the systems in block diagonal form, with $\mathbf{z} = (\mathbf{z}_1, \dots, \mathbf{z}_E)$ and so on. This system is again port-Hamiltonian, with summed-up Hamiltonian function $\mathcal{H}(\mathbf{z}) = \mathcal{H}_1(\mathbf{z}_1) + \dots + \mathcal{H}_E(\mathbf{z}_E)$. The system is still formally not closed, since the input variables are still inputs, and the relations between quantities at the junctions have not been introduced yet.

Because of our standard choice of boundary input operator, the input vector $\mathbf{u} \in \mathbb{R}^{2E}$ contains the momentum at the two ends of each pipe, with the sign chosen so that a positive momentum corresponds to gas flowing towards the interior of the pipe. The output vector $\mathbf{y} \in \mathbb{R}^{2E}$ contains a non-signed[3] quantity, corresponding to the state of the gas at the two ends of each pipe, but with a specific formula depending on the model.

Let us consider the special incidence matrix $A \in \mathbb{R}^{V \times 2E}$, where

$$A_{ik} = \begin{cases} +1 & \text{if the junction } v_i \text{ is touched by the edge end corresponding to } u_k, \\ 0 & \text{otherwise.} \end{cases}$$

Note that A differs from the usual incidence matrix of a graph (which would be of dimension $V \times E$) because each edge is counted once per each end.

Because of conservation of mass, the total gas flow entering a junction must be the same as the total gas flow leaving the junction; this property is equivalent to $A\mathbf{u} = 0$ (Kirchhoff's first law). To guarantee conservation of energy in the interconnected system (i.e., that there is no energy loss at the junctions), we require that the quantity defining $\mathbf{y}$ is continuous along the whole network, i.e., if two output entries y_a, y_b correspond to two pipe ends meeting at the same junction, we force $y_a = y_b$. Equivalently, if λ_i denotes the value of that quantity in the junction v_i, for $i = 1, \dots, V$, we are requesting $\mathbf{y} = A^T\boldsymbol{\lambda}$ (Kirchhoff's second law).

Adding the new algebraic equation $A\mathbf{u} = 0$, introducing $\boldsymbol{\lambda} \in \mathbb{R}^V$ as a new variable, and replacing $\mathbf{y}$ with $A^T\boldsymbol{\lambda}$ in the output equation, the aggregate pH system is so transformed:

$$\begin{bmatrix} \mathbf{E} & 0 & 0 \\ 0 & 0 & 0 \\ 0 & 0 & 0 \end{bmatrix} \begin{bmatrix} \dot{\mathbf{z}} \\ \dot{\mathbf{u}} \\ \dot{\boldsymbol{\lambda}} \end{bmatrix} = \begin{bmatrix} \mathbf{J}(\mathbf{z}) - \mathbf{R}(\mathbf{z}) & \mathbf{G} & 0 \\ -\mathbf{G}^T & 0 & A^T \\ 0 & -A & 0 \end{bmatrix} \begin{bmatrix} \mathbf{e}(\mathbf{z}) \\ \mathbf{u} \\ \boldsymbol{\lambda} \end{bmatrix}, \tag{109}$$

which together with the aggregate Hamiltonian function $\mathcal{H}(\mathbf{z})$ is a dissipative Hamiltonian descriptor system, i.e., it has no external ports.

[3] In the sense that the sign is the same for both ends of the corresponding pipe.

Note that, for some of the simpler models ((ISO3), (ISO4)), requiring the continuity of the output-related quantity is equivalent to require the continuity of the pressure. Nevertheless, the condition $\mathbf{y} = A^T \boldsymbol{\lambda}$ is necessary to preserve the port-Hamiltonian structure. On the other hand, for the models with the alternative pH formulation ((ISO2b),(ISO3b), (ISO4b)), the output-related quantity is exactly the pressure. For the remaining models ((TA1), (TA2), (TA3), (TA4), and (ISO1)), requiring the continuity of the pressure would break the conservation of total energy in the system.

References

[1] Martin Arnold, Karl Strehmel, and Rüdiger Weiner. Half-explicit Runge-Kutta methods for semi-explicit differential equations of index 1. *Numer. Math.*, 64:409–431, 1993.

[2] Pia Bales. Hierarchische Modellierung der Eulerschen Flussgleichungen in der Gasdynamik. Diplomarbeit, Technische Universität Darmstadt, Fachbereich Mathematik, Darmstadt, Juli 2005.

[3] Peter Benner, Sarah Grundel, Christian Himpe, Christoph Huck, Tom Streubel, and Caren Tischendorf. Gas network benchmark models. In Stephen L. Campbell, Achim Ilchmann, Volker Mehrmann, and Timo Reis, editors, *Applications of Differential-Algebraic Equations: Examples and Benchmarks*, pages 171–197. Springer International Publishing, 2019.

[4] R. Boberg, M. Engshuber, and J. Garstka. *Erdgas. Bereitstellung, Anwendung, Umwandlung.* Deutscher Verlag für Grundstoffindustrie, Leipzig, 1974.

[5] J. Brouwer, I. Gasser, and M. Herty. Gas pipeline models revisited: Model hierarchies, nonisothermal models, and simulations of networks. *Multiscale Modeling & Simulation*, 9(2):601–623, 2011.

[6] Günter Cerbe. *Grundlagen der Gastechnik.* Hanser, 2008.

[7] Ning Hsing Chen. An explicit equation for friction factor in pipe. *Industrial & Engineering Chemistry Fundamentals*, 18(3):296–297, 1979.

[8] J. Cheng and C.-W. Shu. High order schemes for cfd: A review. *Chinese Journal of Computational Physics*, 26:636–655, 2009.

[9] B. Cockburn, G. Karniadakis, and C.-W. Shu, editors. *Discontinuous Galerkin Methods: Theory, Computation and Applications*, volume 11 of *Lecture Notes in Computational Science and Engineering.* Springer, 2000.

[10] P. Domschke, B. Geißler, O. Kolb, J. Lang, A. Martin, and A. Morsi. Combination of nonlinear and linear optimization of transient gas networks. *INFORMS J. Comp.*, 23:605–617, 2011.

[11] P. Domschke, B. Hiller, J. Lang, and C. Tischendorf. Modellierung von Gasnetzwerken: Eine Übersicht. Preprint, TRR 154, 2017.

[12] Pia Domschke. *Adjoint-Based Control of Model and Discretization Errors for Gas Transport in Networked Pipelines*. Dissertation, TU Darmstadt, 2011.

[13] J.A. Ekaterinaris. High-order accurate, low numerical diffusion methods for aerodynamics. *Progress in Aerospace Sciences*, 41:192–300, 2005.

[14] E. J. Finnemore and J. E. Franzini. *Fluid Mechanics with Engineering Applications*. McGraw-Hill, 10th edition, 2002.

[15] Edwige Godlewski and Pierre-Arnaud Raviart. *Numerical Approximation of Hyperbolic Systems of Conservation Laws*, volume 118 of *Applied Mathematical Sciences*. Springer Verlag, 1996.

[16] B. Hiller and T. Walther. Modelling compressor stations in gas networks. Technical report, Zuse Institute Berlin, 2017. Fortgeschriebenes Arbeitspapier.

[17] Honeywell. Unisim design. Operations Guide, 2010.

[18] Christoph Huck. *Perturbation analysis and numerical discretisation of hyperbolic partial differential algebraic equations describing flow networks*. Dissertation, Humboldt-Universität zu Berlin, 2018.

[19] Willem Hundsdorfer and Jan G. Verwer. *Numerical Solution of Time-Dependent Advection-Diffusion-Reaction Equations*, volume 33 of *Computational Mathematics*. Springer Verlag, 2003.

[20] Thorsten Koch, Benjamin Hiller, Marc E. Pfetsch, and Lars Schewe, editors. *Evaluating Gas Network Capacities*. MOS-SIAM Series on Optimization. SIAM, 2015.

[21] O. Kolb. *Simulation and Optimization of Gas and Water Supply Networks*. Dissertation, Technische Universität Darmstadt, 2011.

[22] O. Kolb, J. Lang, and P. Bales. An implicit box scheme for subsonic compressible flow with dissipative source term. *Numerical Algorithms*, 53(2):293–307, 2010.

[23] Thomas Kästner, Andreas Kießling, and Gerrit Riemer. *Energie in 60 Minuten. Ein Reiseführer durch die Gaswirtschaft*. VS Verlag für Sozialwissenschaften, 2011.

[24] Randall J. Le Veque. *Finite Volume Methods for Hyperbolic Problems*. Cambridge University Press, 2002.

[25] H. Liu. *Analysis and Numerics for Conservation Laws, G. Warnecke (ed.)*, chapter Relaxation Dynamics, Scaling Limits and Convergence of Relaxation Schemes, pages 453–478. Springer, 2005.

[26] LIWACOM Informationstechnik GmbH. SIMONE software. http://www.liwacom.de/index.php?id=236. Zuletzt besucht: 18. Sep. 2013.

[27] Volker Mehrmann and Riccardo Morandin. Structure-preserving discretization for port-Hamiltonian descriptor systems. In *2019 IEEE 58th Conference on Decision and Control (CDC)*, pages 6863–6868, Nice, France, 2019.

[28] E. Shashi Menon. *Gas Pipeline Hydraulics*. Taylor & Francis Group, 2005.

[29] Riccardo Morandin. Infinite-dimensional port-Hamiltonian descriptor systems. *In preparation*, 2020.

[30] H. Nessyahu and E. Tadmor. Non-oscillatory central differencing for hyperbolic conservation laws. *J. Comput. Physics*, 87:408–463, 1990.

[31] Andrzej J. Osiadacz. Different transient models – limitations, advantages and disadvantages. PSIG report 9606, Pipeline Simulation Interest Group, 1996.

[32] Andrzej J. Osiadacz and Maciej Chaczykowski. Verification of transient gas flow simulation model. PSIG report 1010, Pipeline Simulation Interest Group, 2010.

[33] I. Papay. Ogil musz. tud. kozl., 1968.

[34] Marc E. Pfetsch, Armin Fügenschuh, Björn Geißler, Nina Geißler, Ralf Gollmer, Benjamin Hiller, Jesco Humpola, Thorsten Koch, Thomas Lehmann, Alexander Martin, Antonio Morsi, Jessica Rövekamp, Lars Schewe, Martin Schmidt, Rüdiger Schultz, Robert Schwarz, Jonas Schweiger, Claudia Stangl, Marc C. Steinbach, Stefan Vigerske, and Bernhard M. Willert. Validation of nominations in gas network optimization: Models, methods, and solutions. *Optimization Methods and Software*, 30(1):15–53, 2015. www.optimization-online.org/DB_HTML/2012/11/3694.html.

[35] Dieter Rist. *Dynamik realer Gase: Grundlagen, Berechnungen und Daten für Thermogasdynamik, Strömungsmechanik und Gastechnik*. Springer, 1996.

[36] Martin Schmidt, Marc C. Steinbach, and Bernhard M. Willert. High detail stationary optimization models for gas networks. *Optimization and Engineering*, 16(1):131–164, 2015.

[37] Donald W. Schroeder. A tutorial on pipe flow equations. PSIG report 0112, Pipeline Simulation Interest Group, 2001.

[38] Chi-Wang Shu. Essentially non-oscillatory and weighted essentially non-oscillatory schemes for hyperbolic conservation laws. In Alfio Quarteroni, editor, *Advanced Numerical Approximation of Nonlinear Hyperbolic Equations*, volume 1697 of *Lecture Notes in Mathematics*, pages 325–432. Springer Berlin Heidelberg, 1998.

[39] Joel Smoller. *Shock Waves and Reaction-Diffusion Equations*, volume 258 of *Grundlehren der mathematischen Wissenschaften*. Springer Verlag, 1983.

[40] Erich Truckenbrodt. *Lehrbuch der angewandten Fluidmechanik*. Springer, 1988.

[41] B. Wendroff. On centered difference equations for hyperbolic systems. *J. Soc. Ind. Appl. Math.*, 8:549–555, 1960.